



Geospatial delineation of groundwater recharge potential zones in the Deccan basaltic province, India

Rajarshi Saha¹ · Tushar Wankhede¹ · Iswar Chandra Das¹ · Vinod Kumar Kumaranchat¹ · Satyanarayana Kurry Reddy²

Received: 16 June 2022 / Accepted: 2 March 2023 / Published online: 27 March 2023
© Saudi Society for Geosciences and Springer Nature Switzerland AG 2023

Abstract

The water-scarce drought-prone Manjeera basin, of the Deccan basaltic province, is facing the relentless threat of groundwater over-exploitation. This region needs a reliable strategy to overcome groundwater scarcity as this province is of great hydrogeological significance. There is a deficiency of dependable information about the groundwater recharge potential zone (GWRPZ) for this province. Groundwater recharge (GWR) is vital for creating a balance in water resources. With the aim of solving this severe water crisis, this study was conducted. This study is a very potent hybrid approach of satellite imagery and digital elevation model along with other ancillary data analysis using ArcGIS software geospatial platform with multi-criteria decision analysis (MCDA) driven analytical hierarchy process (AHP) and multi-influencing factor (MIF) models for GWRPZ map delineation. Crucial hydrogeological variables were utilized to achieve an efficient GWRPZ map for effective artificial recharge planning. The derived maps were classified into four distinct zones, viz. very good, good, moderate and poor. Critical parameters like branching factor (BF) (0.16 and 0.12), miss factor (MF) (0.11 and 0.26), detection percentage (DP) (89.86% and 79.17%) and overall quality percentage (OQP) (78.48% and 72.15%) demonstrated good prediction accuracy for AHP and MIF respectively. This research output may assist the planners/policymakers/local administration in precise groundwater development and recharge strategies to achieve a sustainable groundwater development scenario.

Keywords Groundwater recharge · AHP · MIF · Geospatial · Sustainable development

Introduction

Groundwater overexploitation is a threat to the earth's sustainability, which unsettles the balance of groundwater resources (Ostad-Ali-Askari et al. 2017; Nithya et al. 2019). The rapid growth of population, urbanization, industrialization and drastic increase in the irrigation sector contributed towards groundwater over-exploitation leading to groundwater stress. In the twenty-first century, water security is likely to be the biggest challenge for mankind and its well-being (Bogardi et al. 2012). India is the largest groundwater exploiter in the world and exploits more than 25% of the total world's exploited groundwater (Bali et al. 2015). More than 60% of irrigation in India is through groundwater, and around 90% of rural and 30% of the urban population's drinking/domestic need is fulfilled by it (Pius et al. 2012; Saha et al. 2021). Groundwater, as a cheap/reliable source, is abstracted indiscriminately, causing its overexploitation in several parts of India (CGWB 2017a). Groundwater over-exploitation, without considering the recharging capabilities of aquifers and other geo-environmental factors, has resulted

Responsible Editor: Broder J. Merkel

✉ Rajarshi Saha
rajarshigeology@gmail.com

Tushar Wankhede
tushar1771@gmail.com

Iswar Chandra Das
icdasiirs@gmail.com

Vinod Kumar Kumaranchat
vinodkumar_k@nrsc.gov.in

Satyanarayana Kurry Reddy
snrkurrys@rediffmail.com

¹ Geosciences Group, National Remote Sensing Centre, ISRO, Hyderabad, India

² Department of Geology, College of Science & Technology, Andhra University, Visakhapatnam 530 003, India

in a drastic decline in the groundwater table, i.e. around 12 to 15 m on average and up to 25 m in some areas (Mathai et al. 2015). In addition, diverse hydrogeological conditions associated with uneven monsoon patterns in India deprive the aquifers of substantial groundwater recharge (GWR) (Eslamian et al. 2018; Saha et al. 2018). Moreover, the population growth rate and associated water demand will further aggravate water scarcity in the near future (Abijith et al. 2020). Therefore, GWR is crucial to maintaining a balance between groundwater resources and exploitation towards water security and sustainable groundwater management. Thus, any sustainable groundwater management strategies must incorporate GWR measures based on the regional hydrogeological settings and associated controlling factors (Dharpure et al. 2021). Delineation of GWRPZ is very crucial in this aspect, which leads to the stoppage of further declination of the groundwater table by replenishment through implementing artificial recharge measures (Eslamian et al. 2018; Etikala et al. 2019; Singh et al. 2019). As an important aspect of the hydrological cycle, GWR is dynamic, interdisciplinary and controlled by geomorphology, lineament, lithology, landuse, slope, soil, drainage and rainfall (Shekhar and Pandey 2015; Ostad-Ali-Askari et al. 2017; Chaudhry et al. 2019).

Advancement and modernization of geospatial techniques are very effective and efficient in mapping, monitoring and modelling key natural resources (Singh et al. 2013; Singha et al. 2019). The integrated approach of remote sensing (RS), geographical information system (GIS) using earth observation (EO) satellite imagery, field and ancillary data is well established in a wide spectrum of groundwater management studies (Sahoo et al. 2017; Chaudhry et al. 2019). Conventional RS-GIS application for GWRPZ yielded positive results and has been used extensively in the recent past (Avtar et al. 2010; Mishra et al. 2010). Index-dependent modelling studies for GWRPZ are emerging as very powerful techniques for effective groundwater management strategies (Khan et al. 2020; Kadam et al. 2021). Several types of methods and models were adopted to carry out GWRPZ, namely analytical hierarchy process (AHP) (Kaliraj et al. 2014; Jena et al. 2020), multi-influencing factor (MIF) (Pande et al. 2020; Zghibi et al. 2020), weighted sum overlay analysis (WTSOA) (Patra et al. 2018; Andualem and Demeke 2019), fuzzy model (Mohamed and Elmahdy 2017; Gesim and Okazaki 2018), frequency ratio and certainty factor (Razandi et al. 2015; Razavi-Termeh et al. 2019), random forest model (Rahmati et al. 2016; Norouzi and Shahmohammadi-Kalalagh 2019), and artificial neural network (Chen et al. 2021; Tamiru and Wagari 2021). By the works carried out in the last one and half decades, it has been seen that MCDA is a significantly powerful method for understanding groundwater management framework. The

AHP is a GIS-based, very effective and favoured MCDA technique, which uses the pairwise comparison of different spatial thematic variables as per assigned distinctive weightage, based on domain knowledge and expert opinion (Dar et al. 2020; Javadi et al. 2021). The MIF is an efficient MCDA technique. It calculates the inter-relationship between the different thematic variables, as per the assigned weights by domain experts, depending on the major and minor influencing factors towards GWR (Etikala et al. 2019; Zghibi et al. 2020). With time progression, AHP and MIF, in combination with WTSOA gained a reputation due to usefulness, simplicity, quick, effective and practical solutions for groundwater resource management in diverse hydrogeological provinces before conducting expensive field explorations (Andualem and Demeke 2019; Abijith et al. 2020).

India demonstrates a distinct and unique province-wise groundwater regime due to its varied hydrogeological and geo-environmental settings. Therefore, groundwater researchers relentlessly face the challenge for precise delineation of GWRPZ and understanding the controlling spatio-temporal variable factors. Thus, this AHP and MIF MCDA model applicability needs to be evaluated in complex hydrogeological terrains spreading across Pan India like Deccan basaltic province. Moreover, reliable GWRPZ researches in this water-scarce drought-prone Manjeera basin of the Deccan basaltic province are very rare. Even though this basin holds greater importance, as a major part of the Godavari basin of India, however, it lacks dependable information about GWRPZ and needs attention as this province is known for its harsh hydrogeological and geo-environmental condition. GWRPZ delineation will significantly improve groundwater sustainability and water security in this region. This will also act as a guideline for water scarcity in drought-prone areas in the country, since the present study area is a severe drought-prone, hard rock basaltic province and facing relentless water shortage for quite a few years (CGWB 2017b, 2020 and 2021; Navane and Sahoo 2021). It is anticipated that water scarcity will further aggravate due to groundwater over-exploitation in combination with declining rainfall and associated hydrogeological behaviour of the basaltic aquifers. Therefore, in this present research, AHP and MIF, in combination with the WTSOA modelling approach, were used in ArcGIS geospatial platform for deriving GWRPZ and GWRPZI in a hard rock basaltic terrain with the following objective. The objective deals with generating a GWRPZ map to improve groundwater resource management by GWR for long-term groundwater sustainability and water security. The robustness and accuracy of the work are validated using pre and post-monsoon water table fluctuation data in combination with model output-derived metrics (Shufelt 1999; Lee et al. 2003; Marta et al. 2012a).

Materials and methods

Study area

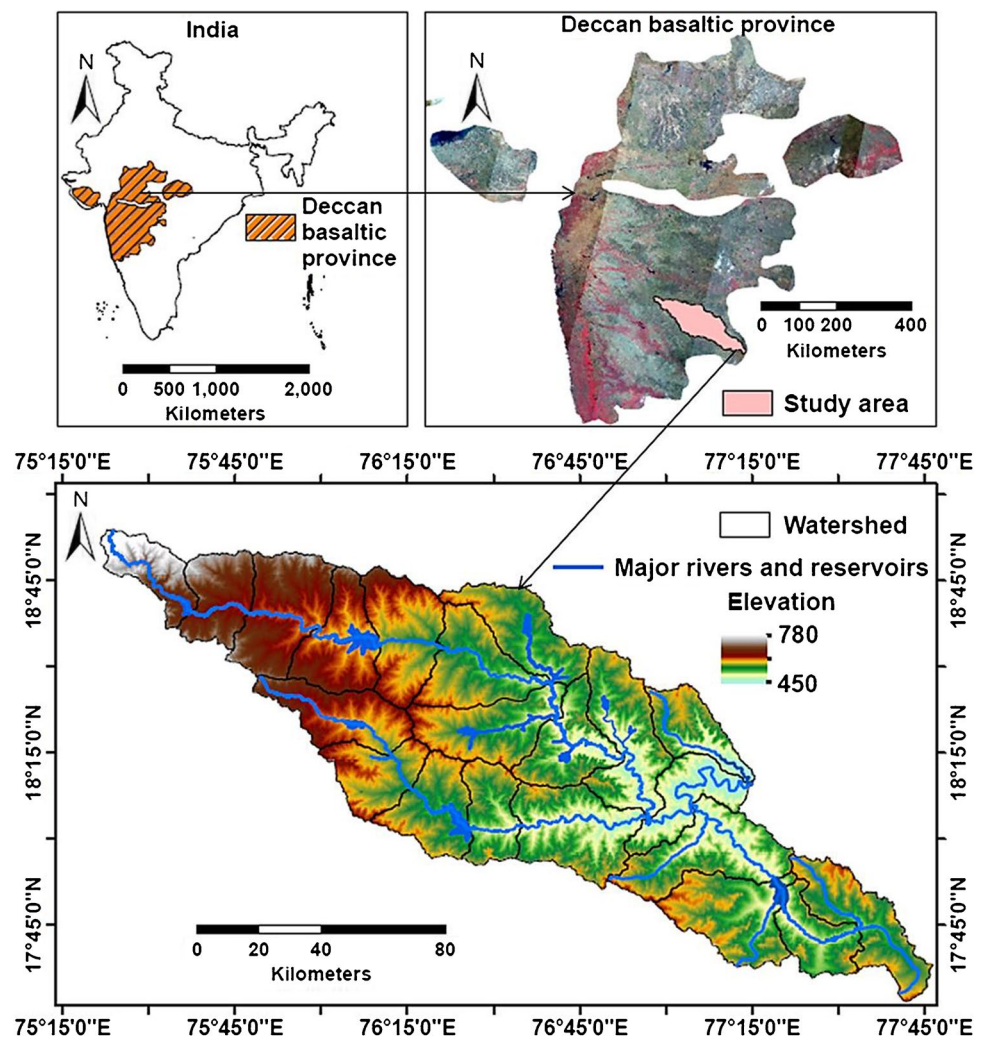
The study area is a part of the Manjeera basin of the Deccan basaltic province, which spread across three states of India, namely Maharashtra, Karnataka and Telangana, with a population of around 180 million (Census 2011). The study area consists of a total of twenty-one major watersheds, covering an area of approximately 14,010 km² (CWC 2014). It is located between latitude 17°31'00" N to 18°54'00" N and longitude 75°21'00" E to 77°47'00" E (Fig. 1). Manjeera, Dev, Dodda-Halla, Karania, Chulki, Madhura and Trina are the rivers within the study area. The majority of the study area is represented by single crop, double/triple crop and agricultural fallow land land-use classes. This study area witnesses a hot and dry climate with temperatures ranging from 12 to 42 °C (CGWB 2012, 2013 and 2014) and rainfall ranging from 715 to

897 mm. The elevation of the study area ranges from 450 to 780 m. The majority of the study area represents low to moderate groundwater yield, except few areas where the yield is good.

Groundwater scenario in the recent past

This study area has been consistently battling severe water scarcity for more than a decade. The severity is far worse in the western part, as it is the upper catchment of the Manjeera basin where surface water availability is scarce (Edge 2015). Therefore, groundwater plays a pivotal role in meeting most of the huge water demand for this region due to booming agriculture and population (GSDA 2012; Edge 2015). The stage of groundwater development is very high in this region (more than 75%) (CGWB 2012, 2013). During summer, almost all the surface water bodies dry up, and groundwater wells mostly become defunct or work with very less yield due to the drastic decline of the water table (CGWB 2020 and 2021). The water scarcity reached such a stage in 2016

Fig. 1 Location map showing the study area, part of the Manjeera basin in the Deccan basaltic province



to fulfil the needs of water brought by train from a considerable distance (Osmani and Patil 2019). This nature of water scarcity is very alarming, and it affects the resident population of this province very badly.

Methodology

Data sources, selection and generation of hydrogeological thematic layers

A total of eight thematic layers were considered to delineate the GWRPZ zone. These are geomorphology, lineament, lithology, landuse, slope, soil texture, drainage and rainfall. These thematic variables are the controlling factor for groundwater storage and movement within the study area, therefore controlling the GWR of the province. Lithology and geomorphology thematic maps were modified from the existing database. In contrast, lineament, drainage and slope were delineated using Resourcesat-2 linear imaging self-scanning (LISS) III satellite image (30 m spatial resolution), Cartosat-1 digital elevation model (DEM) (30 m posting) with other available thematic layers. Image enhancing techniques were implemented on the satellite images and image draping over DEM to bring out the best possible result while modifying/delineating the thematic variables using image processing and analysis software ENVI® and ArcGIS. Furthermore, landuse and soil texture maps were used as they are from the existing database. All these thematic variables were rasterized and re-projected into UTM projection, WGS-84 datum in Zone 43N using ArcGIS platform with a spatial resolution of 30 m. A rainfall map was also prepared using the ArcGIS platform with the exact specifications.

The geomorphology layer was modified from National Rural Drinking Water Programme (NRDWP) maps available in the bhuvan-bhujal portal (<https://bhuvan.nrsc.gov.in/>) by integrated use of satellite imagery and DEM (Martha et al. 2012b). Precise boundary modification of different geomorphic landforms from the existing database was carried out using satellite images and DEM's spectral contrast and spatial characteristics. Using image processing and analysis software ENVI® principal component analysis (PCA) was carried out on visible-near infrared (VNIR) and short wave infrared (SWIR) bands, and different false colour composite (FCC) images were created. These PCA and satellite FCC images were used to accurately bring out the boundaries of different plateaus and lateritic plains based on spectral contrast of weathering and overburdened material. Moreover, PCA inputs were used to improve the decorrelative information of spectral bands (Gupta 2003). Furthermore, image draping over the DEM created a three-dimensional perspective visualization, which eventually helped in precise boundary modification of butte, and mesa from the plateaus. RS image interpretation fundamental elements such as shape,

size, tone, texture, shadow, pattern and association were also provided with both qualitative and quantitative knowledge for delineating different geomorphic landforms (Bennia et al. 2013). The lithology layer was recreated from the NRDWP bhuvan-bhujal portal (<https://bhuvan.nrsc.gov.in/>) available maps along with the help of spectral signature variability of satellite imagery (Guha et al. 2018). These available maps were used as reference data, and thereafter, the boundary of the basalt and laterite was modified using different FCC band combinations of satellite imagery and PCA images. It was noticed that the variable combinations of RGB of different PCA and satellite image bands helped enhance the lithological variations, which eventually helped in accurately modifying the lithological boundaries. Similarly, spectral contrast of the different FCC band combinations in combination with landuse information also helps in precisely modifying the lithological boundary. Lineaments were delineated in the ArcGIS platform using FCC satellite images and DEM conjugally (Dasgupta and Mukherjee 2019). Visual interpretations and automated digital techniques were used for lineament detection and identification. The first method was carried out depending upon the amalgamation of crucial RS aspects like shape, size, tone, texture and association. The edge detection technique using high pass filtering applied the second automated method. The artifices from the automated techniques were later corrected manually, some of which may be developed due to variable illumination, shadow, association and topology (Gupta 2003). These lineaments were cross-checked in the field and from National Geomorphological and Lineament Mapping (NGLM) database from the Bhuvan portal (<https://bhuvan.nrsc.gov.in/>), wherever it was possible. Then, this lineament layer was used to generate lineament density using tools of ArcGIS software using line density tool. Similarly, by applying visual interpretation techniques depending upon the integrated key RS objects of satellite imagery and DEM, drainages were delineated in ArcGIS (Mukherjee et al. 2012). Drainages were also delineated in an automated manner from Cartosat 1 DEM using ArcGIS spatial analyst toolbox. In a step-by-step process from Cartosat 1 DEM fill sink, flow direction, flow accumulation, conditioning, stream ordering and then stream shape file were generated. These drainage shape files were validated using the India Water Resource Information System portal (<https://indiawris.gov.in/>). After that, using the line density tool in ArcGIS, drainage density is delineated. The landuse map (2018–2019) used in this research was used as it is from National Remote Sensing Centre's Bhuvan portal (<https://bhuvan.nrsc.gov.in/>). These maps have an overall classification accuracy of around 90%, with a range of 86 to 95% (<https://bhuvan-app1.nrsc.gov.in/>; NLULC 2007). As these are already published maps with accuracy estimation, any separate accuracy assessment was not carried out. Cartosat-1 DEM of 30 m posting was used to generate a slope

map in degrees (°) using ArcGIS software 3D analyst tools. Soil map was directly used from the National Bureau of Soil Survey and Land Use Planning (NBSS&LUP) published soil map (<https://www.nbsslup.in/>). India Meteorological Department (IMD) gridded rainfall data (<https://www.imdpu.ne.gov.in>) of the last 26 years from 1995 to 2020 was used for the yearly rainfall average to generate a rainfall map. A total of 33 point locations were created from the gridded rainfall data by taking the centre of the grid as the point locations. Then the rainfall distribution map was prepared, using spatial interpolation technique, inverse distance weighting (IDW) in ArcGIS software with 12 neighbourhood points with variable search radius. This technique predicts the values of the variables at unobserved locations by using the spatial correlation of the variables (Murmu et al. 2019). This technique is very potent in predicting spatial distribution depending on the sample point’s availability and suitable spatial distribution.

Furthermore, all these thematic layers were assigned weightage, and their corresponding classes were assigned rank as per their influence towards GWR. These weightages were given using AHP and MIF techniques, followed by a ranking of classes as per the domain knowledge, previous literature and subject experts’ know-how. All these thematic layers’ weightage and rank hierarchy represent favourability towards the GWR of that particular theme and corresponding classes respectively. Later, WTSOA was executed by integrating all eight thematic layers for GWRPZ map generation and GWRPZI computation.

A detailed conceptual framework methodology of this research is given in Fig. 2.

Normalized weight computation of thematic layers using AHP

AHP is a widely followed, effective decision-making tool, proposed by Saaty (1980, 2005) depending upon the multi-criteria approach. This approach eases the difficulty of any complex decision by assigning weights to different themes to formulate a hierarchical structure amongst them (Kumar and Krishna 2018; Aju et al. 2021). AHP is a very powerful and robust method for multi-criteria assessment by integrating domain knowledge with practical practices (Chowdhury et al 2010; Das and Pal 2020). However, for AHP execution and precise object-oriented result generation, the weight assigning along with weight normalization is a very important part (Shekhar and Pandey 2015; Nithya et al. 2019). AHP is a step-by-step methodical approach which includes a pairwise comparison matrix (PCM), normalized pairwise matrix (NPM) formulation, normalized weight computation and consistency checking (Kumar et al. 2014; Arulbalaji et al. 2019). These computations were carried out using Microsoft Excel ©

software. Therefore, in this study, utmost care was taken before relative weight was assigned to each thematic layer with respect to other themes in the formulation of PCM. The weights were assigned as per domain knowledge, field experience and expert hydrogeologist’s opinion, along with plenty of existing literature careful, detailed review and evaluation (Arulbalaji et al. 2019; Bhattacharya et al. 2020; Dar et al. 2020).

The interrelationship amongst the thematic layers was computed using Saaty’s scale of relative importance on a scale of 1 to 9, where 1 demonstrates equal importance and 9 demonstrates extreme importance amongst each theme (Table 1) (Saaty 1980, 2005). Thus, the PCM was prepared (Eq. 1) based on each thematic layer’s interrelationship with another thematic layer (Table 2) (Singh et al. 2013; Murmu et al. 2019).

$$A = [X_{ij}] = \begin{bmatrix} X_{11} & X_{12} & \dots & X_{1n} \\ X_{21} & X_{22} & \dots & X_{2n} \\ \dots & \dots & \dots & \dots \\ X_{n1} & X_{n2} & \dots & X_{nn} \end{bmatrix} \tag{1}$$

where A is PCM; X_{nn} is the relative significance of a thematic variable, when compared to another parameter towards GWR; $X_{11}, X_{22}, \dots, X_{nn} = 1$; where $i, j = 1, 2, \dots, n$; and $X_{ij} = 1/X_{ji}$.

In the next step, NPM was computed (Eq. 2), where each PCM theme’s particular column values were divided by the corresponding column sum to obtain the NPM themes (Table 2).

$$X_{ij} = \frac{Y_{ij}}{Z_j} \tag{2}$$

where X_{ij} is the NPM value at the i th row and j th column; Y_{ij} is the value at the i th row and j th column in PCM; Z_j is the column sum of the j th column in PCM.

From Table 2, the normalized weight for each theme towards GWR is computed as the sum of all elements of a particular row divided by the number of cells in the same row of NPM (Eq. 3)

$$W_i = \frac{\sum X_{ij}}{N} \tag{3}$$

where W_i is the normalized weight; N is the total number of themes.

The next step involved was principal eigenvalue (λ_{max}) calculation (Eqs. 4.1-4.5), which is required for consistency checking (Kumar et al. 2014; Jhariya et al. 2021).

$$A * \begin{bmatrix} W_1 \\ W_2 \\ \dots \\ W_n \end{bmatrix} \tag{4.1}$$

Fig. 2 Schematic design of the methodology adopted in this research

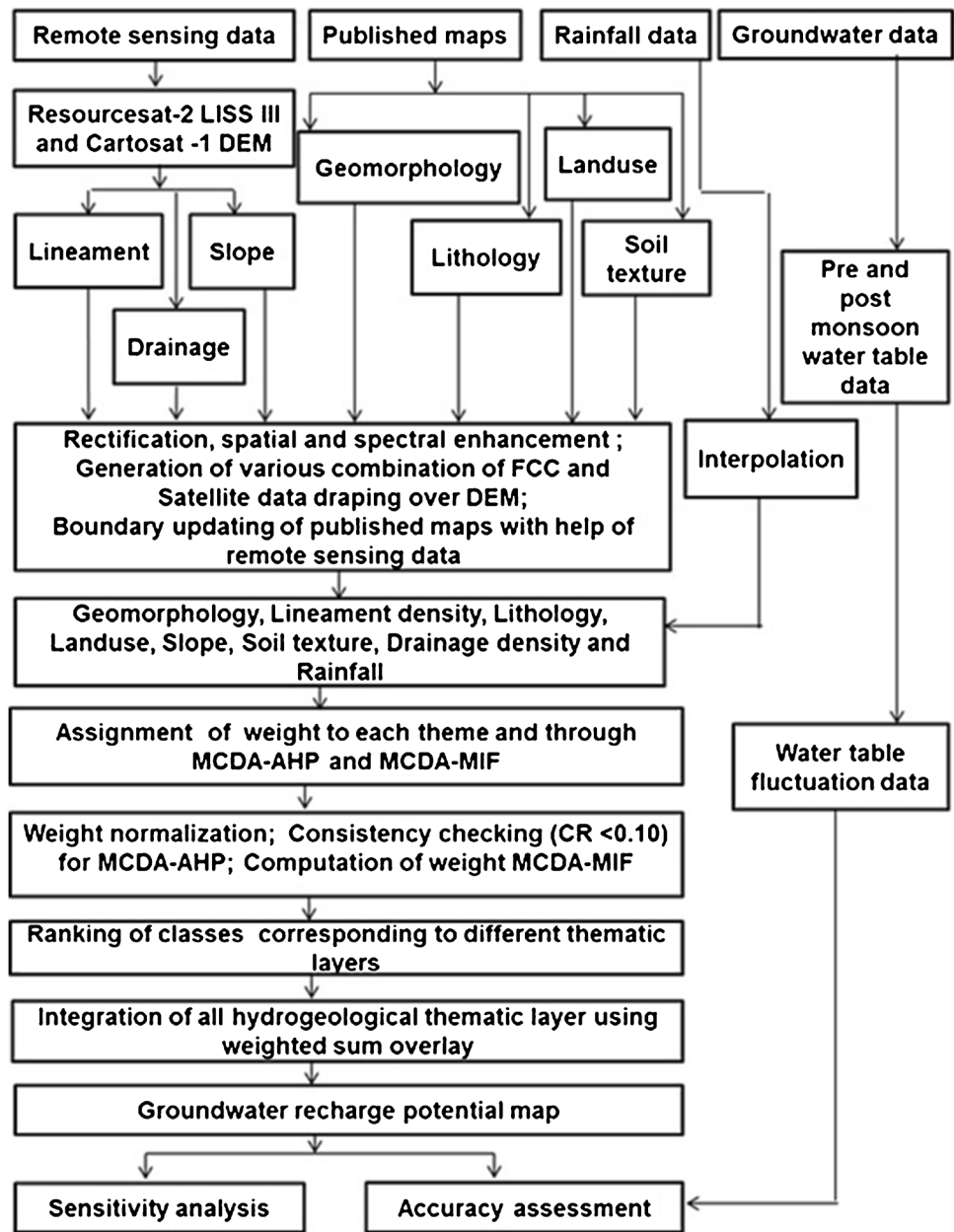


Table 1 Saaty’s AHP scale of relative importance (1–9) and ratio index (RI) for the different *n* numbers (Saaty 1980, 2005), where *n* is the number of the variable used

Scale	1	2	3	4	5	6	7	8	9
Intensity of importance	Equal	Equal to moderate	Moderate	Moderate to strong	Strong	Strong to very strong	Very strong	Very strong to extreme	Extreme
<i>n</i> (number of variable used)	1	2	3	4	5	6	7	8	9
	1/9	1/8	1/7	1/6	1/5	1/4	1/3	1/2	1
									2
									3
									4
									5
									6
									7
									8
									9
	← Less important					More important →			
RI values	0	0	0.58	0.90	1.12	1.24	1.32	1.41	1.45

Table 2 Pair-wise comparison matrix for eight thematic layers, normalized pairwise matrix, the normalized weight (NW) of each thematic layer, principal eigenvalue, consistency index and consistency ratio

Pair-wise comparison matrix									
Thematic layers	GM	LD	LT	LU	SL	ST	DD	RF	
GM (geomorphology)	1.00	2.00	3.00	4.00	5.00	6.00	7.00	8.00	
LD (lineament density)	0.50	1.00	2.00	3.00	4.00	5.00	6.00	7.00	
LT (lithology)	0.33	0.50	1.00	2.00	3.00	4.00	5.00	6.00	
LU (landuse)	0.25	0.33	0.50	1.00	2.00	3.00	4.00	5.00	
SL (slope)	0.20	0.25	0.33	0.50	1.00	2.00	3.00	4.00	
ST (soil texture)	0.17	0.20	0.25	0.33	0.50	1.00	2.00	3.00	
DD (drainage density)	0.14	0.17	0.20	0.25	0.33	0.50	1.00	2.00	
RF (rainfall)	0.13	0.14	0.17	0.20	0.25	0.33	0.50	1.00	
SUM	2.72	4.59	7.45	11.28	16.08	21.83	28.50	36.00	
Normalized pairwise matrix (NPM)									
Thematic layers	GM	LD	LT	LU	SL	ST	DD	RF	NW
GM (geomorphology)	0.37	0.44	0.40	0.35	0.31	0.27	0.25	0.22	0.33
LD (lineament density)	0.18	0.22	0.27	0.27	0.25	0.23	0.21	0.19	0.23
LT (lithology)	0.12	0.11	0.13	0.18	0.19	0.18	0.18	0.17	0.16
LU (landuse)	0.09	0.07	0.07	0.09	0.12	0.14	0.14	0.14	0.11
SL (slope)	0.07	0.05	0.04	0.04	0.06	0.09	0.11	0.11	0.07
ST (soil texture)	0.06	0.04	0.03	0.03	0.03	0.05	0.07	0.08	0.05
DD (drainage density)	0.05	0.04	0.03	0.02	0.02	0.02	0.04	0.06	0.03
RF (rainfall)	0.05	0.03	0.02	0.02	0.02	0.02	0.02	0.03	0.02
$\lambda_{max} = 8.29$			CI=0.04			CR=0.03			

$$A' = \begin{bmatrix} B_{11} & B_{12} & \dots & B_{1n} \\ B_{21} & B_{22} & \dots & B_{2n} \\ \dots & \dots & \dots & \dots \\ B_{n1} & B_{n2} & \dots & B_{nn} \end{bmatrix} \tag{4.2}$$

$$\begin{bmatrix} B_{11} + B_{12} + \dots + B_{1n} \\ B_{21} + B_{22} + \dots + B_{2n} \\ \dots \\ B_{n1} + B_{n2} + \dots + B_{nn} \end{bmatrix} = \begin{bmatrix} S_1 \\ S_2 \\ \dots \\ S_n \end{bmatrix} \tag{4.3}$$

$$\begin{bmatrix} S_1/W_1 \\ S_2/W_2 \\ \dots \\ S_n/W_n \end{bmatrix} = \begin{bmatrix} Y_1 \\ Y_2 \\ \dots \\ Y_n \end{bmatrix} \tag{4.4}$$

$$\lambda_{max} = \frac{Y_1 + Y_2 + \dots + Y_n}{n} \tag{4.5}$$

where A is PCM; W_1, W_2, \dots, W_n is the normalized weight of each of the different thematic variables; A' is the matrix obtained from multiplied PCM with normalized weight; S_1, S_2, \dots, S_n is the row sum of a particular row; Y_1, Y_2, \dots, Y_n is the value obtained from dividing S_1, S_2, \dots, S_n with W_1, W_2, \dots, W_n respectively.

In the next step, the consistency index (CI) (Table 2) was calculated by using the following Eq. 5.

$$CI = \frac{\lambda_{max} - n}{n - 1} \tag{5}$$

where λ_{max} is the principal eigenvalue, and n is the total number of thematic layers used in this study.

This was followed by the computation of consistency ratio (CR) (Table 2), which should be less than 0.1 or 10%; otherwise, the matrix revision is required. The CR is calculated by the following Eq. 6. For this present research, the weights of the thematic layers yielded a CR value of 0.03, which reveals that the assigned weights of different thematic layers are consistent.

$$CR = \frac{CI}{RI} \tag{6}$$

where RI is the ratio index (Table 1).

Weight computation of thematic layers using MIF

MIF is a popular MCDA technique for GWR management studies (Etikala et al. 2019; Abijith et al. 2020). The MIF method is easy, quick and effective for delineating the

appropriate weightage of different thematic layers depending upon their influence on groundwater flow and storage towards GWR. In this research, major and minor influential interrelationship was established in a knowledge-guided domain, amongst the thematic layers. Every interrelationship between the thematic variables was characterized as a major or minor effect based on their strength which controls GWR (Fig. 3). Geomorphology possesses a strong relationship with lithology, landuse, soil and DD, whereas a weak relationship with LD. On the other hand, LD holds a strong relationship with geomorphology, lithology and DD, whereas a weak relationship with landuse. Lithology bears a significant relationship with geomorphology, LD, landuse, soil and a weak relationship with slope. Landuse demonstrates a strong relationship with DD and rainfall, whereas a weak relationship with geomorphology, lithology and slope. Slope, on the other hand, holds a strong relationship with DD, whereas it has a weak relationship with landuse, geomorphology and rainfall. Soil holds a strong connection with landuse and a weak relationship with geomorphology. Furthermore, DD demonstrates a strong relationship with geomorphology, whereas it has a weak relationship with LD and landuse. Rainfall, however, holds a strong and a weak relationship with DD and landuse, respectively. In an interrelationship between thematic variables, if a major effect was present and demonstrated a strong relationship, a weight of 1.0 was assigned. If a minor effect exists between the thematic

variables and establishes a weak relationship, a weight of 0.5 was given. Furthermore, if no effect exists between the thematic variables, a score of 0 was assigned. The relative effect factor for each thematic variable was computed using Microsoft Excel © software from the sum of both major and minor effect weight (Abijith et al. 2020; Zghibi et al. 2020). The relative weight was further used to compute the MIF weight of influence by the following Eq. 7, for each thematic variable towards GWR. Table 3 demonstrates different thematic layers' weights calculated from MIF.

$$MIFW_f = \frac{(E_\alpha + E_\beta)}{\sum_{f=1}^n E_\alpha + E_\beta} * 100 \quad (7)$$

where $MIFW_f$ is the weight influence for the f th theme; E_α and E_β are the major and minor effect factor respectively.

Ranking of classes corresponds to different thematic variables

Assigning rank to different classes of thematic variables in MCDA research is also very important. While assigning the rank, thorough care was adopted, and the rank was assigned as per field knowledge, expert hydrogeologist's opinion and existing literature (Kadam et al. 2020; Navane and Sahoo 2021). The corresponding classes of the theme

Fig. 3 Inter-relationship between the thematic layers influencing GWR, used in MIF

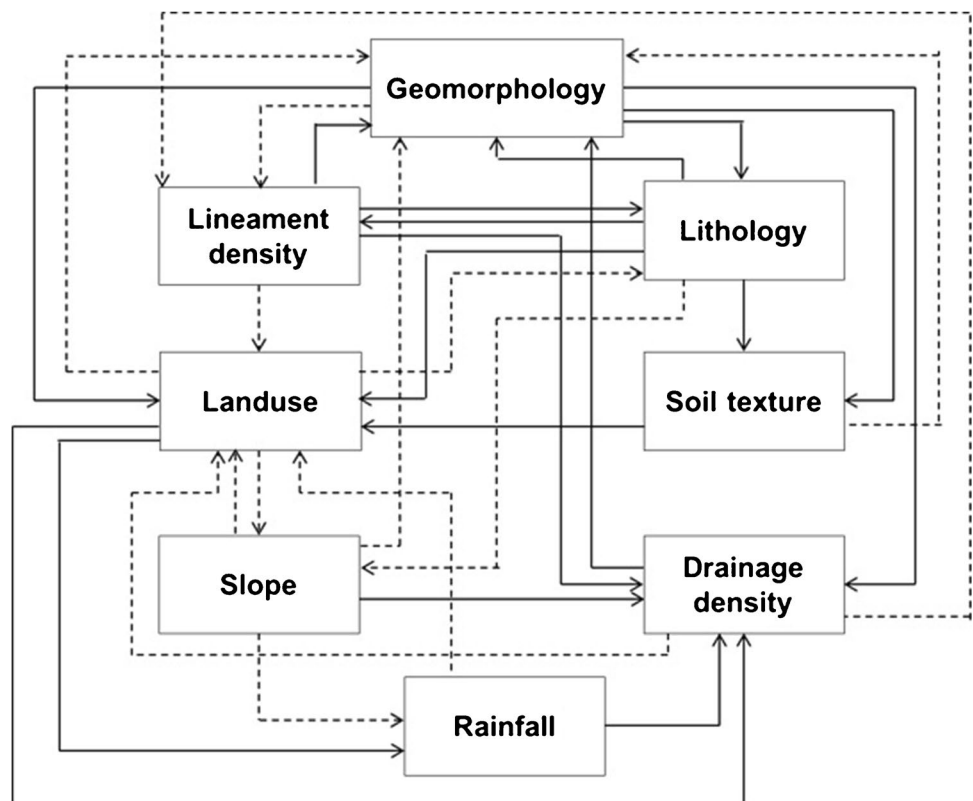


Table 3 The computed weight for MIF, major and minor effect factor for different thematic layers

Thematic layers	Major effect factor	Minor effect factor	Relative factor	Computed weight %	Computed weight factor
Geomorphology	1 + 1 + 1 + 1	0.5	4.5	19	0.19
Lineament density	1 + 1 + 1	0.5	3.5	15	0.15
Lithology	1 + 1 + 1 + 1	0.5	4.5	19	0.19
Landuse	1 + 1	0.5 + 0.5 + 0.5	3.5	15	0.15
Slope	1	0.5 + 0.5 + 0.5	2.5	11	0.11
Soil texture	1	0.5	1.5	6	0.06
Drainage density	1	0.5 + 0.5	2.0	9	0.09
Rainfall	1	0.5	1.5	6	0.06

were provided on a scale of 1 to 9, where 1 is the least and 9 is the extreme value towards GWR, i.e. values closer to 9 indicate favourability of GWR, and closer to 1 indicate non-favourability of GWR.

Groundwater recharge potential zone (GWRPZ) delineation and groundwater recharge potential zone indexing (GWRPZI)

WTSOA is a reproduction technique which generates an integrated map by combining information and geometric properties of different thematic layers in the ArcGIS platform (Mseli et al. 2021). WTSOA reproduces the GWRPZ map depending upon the influence of different hydrogeological thematic layers and their classes. The GWRPZI computed by WTSOA is a dimensionless value representing the probable groundwater recharge zonation spanning over a region (Anduaem and Demeke 2019). GWRPZI can be expressed by Eq. 8 (Malczewski 1999; Kumar and Krishna 2018).

$$GWRPZI = \sum_{m=1}^x \sum_{n=1}^y W_m * RK_n \tag{8}$$

where W_m is the normalized/computed weight factor of the m th thematic layer; RK_n is the rank of the n th class of the thematic layer; x is the total no. of thematic layers; and y is the total number of classes in a given theme.

The GWRPZI can also be represented by Eq. 9 (Agarwal and Garg 2016; Kumar and Krishna 2018).

$$GWRPZI = (GM_w GM_{rk} + LD_w LD_{rk} + LT_w LT_{rk} + LU_w LU_{rk} + SL_w SL_{rk} + ST_w ST_{rk} + DD_w DD_{rk} + RF_w RF_{rk}) \tag{9}$$

where GM is the geomorphology; LD is the lineament density; LT is the lithology; LU is the landuse; SL is the slope; ST is the soil texture; DD is the drainage density; RF is the rainfall. Furthermore, the w and rk subscript represents the normalized/computed weight of a theme and the rank of the theme’s individual features, respectively.

These derived GWRPZI values were used in the classification of the study area into four contrasting GWRPZ, viz. very good, good, moderate and poor.

Sensitivity analysis

The eight thematic variables used in this research demonstrate a variable degree of influence towards GWRPZ. Assigned weights of each thematic layer and the rank of their corresponding classes control the GWPRZ (Lee et al. 2018; Kumar and Krishna 2020). Sensitivity analysis measures the robustness associated with the modelled output in relationship with the input variables. It explains the degree of influence of different thematic variables on the output result by measuring the difference in output result with respect to change of input variables. In this present research, two different procedures of sensitivity analysis were performed to analyse each thematic input variable sensitivity, namely (i) map removal sensitivity analysis (MRSA) (Lodwick et al. 1990) and (ii) single parameter sensitivity analysis (SPSA) (Napolitano and Fabbri 1996).

Map removal sensitivity analysis (MRSA)

MRSA was performed to understand the impact of each thematic layer by removing that thematic layer used in the generation of the GWRPZ map. In this procedure, each of the thematic layers was removed, and with the remaining thematic layers, a new GWRPZ map was created in each

instance. This can be represented with Eq. 10.

$$MRSA_i = \frac{\left| \frac{GWRPZ}{N} - \frac{GWRPZ'}{N'} \right|}{GWRPZ} * 100 \tag{10}$$

where $MRSA_i$ is the map removal sensitivity index; $GWRPZ$ is the groundwater recharge potential zone map obtained using all the thematic variables; $GWRPZ'$ is the groundwater recharge potential zone map obtained by excluding one thematic variable at an instance; N and N' are the number of thematic variables used in obtaining $GWRPZ$ and $GWRPZ'$ map respectively.

Single parameter sensitivity analysis (SPSA)

The SPSA was performed to analyse the control of each thematic layer on the GWRPZ map. This procedure reveals the effective weighting factor of each thematic variable against the assigned weighting factor. This can be expressed using Eq. 11.

$$SPSA_i = \frac{TH_w THC_{rk}}{GWRPZ} * 100 \quad (11)$$

where $SPSA_i$ is the index indicating the effective weighting factor of each thematic layer; TH_w is the assigned weight of each thematic layer, and THC_{rk} is the rank value for each class of thematic layer; $GWRPZ$ is the groundwater recharge potential zone map

Accuracy assessment of the GWRPZ

Accuracy assessment of any simulation model is a very important stage; otherwise, the model remains incomplete. Therefore, establishing the relationship between GWRPZ maps and the actual ground scenario is of great significance for the validation of the work. A total of 79 observation wells, water table fluctuation of pre-monsoon (May 2017) and post-monsoon (November 2017) seasons were used to assess the accuracy of the GWRPZ map (Chowdhury et al. 2010; Kaliraj et al. 2014; Charan et al. 2020).

The accuracy of the output results, derived from AHP and MIF, can be expressed in terms of BF, MF, DP and OQP of the models (Shufelt 1999; Lee et al. 2003; Marta et al. 2012a). This method does a very effective accuracy assessment; thus, it was adopted. The accuracy of this research is expressed by the following Eqs. 12 to 15.

$$BF = \frac{Falsepositive}{Truepositive} \quad (12)$$

$$MF = \frac{False\ negative}{True\ positive} \quad (13)$$

$$DP = 100 * \frac{Truepositive}{(Truepositive + Falsenegative)} \quad (14)$$

$$OQP = 100 * \frac{True\ positive}{(True\ positive + False\ negative + False\ positive)} \quad (15)$$

The BF and MF are the indicators of two potential errors, false positive and false negative, associated with the model at the time of GWRPZ computation. BF provides an overestimation of the GWRPZ, which indicates an incorrect estimation of lower GWRPZ to higher GWRPZ. On the contrary, MF provides an underestimation of GWRPZ, which indicates the estimation of higher GWRPZ to lower GWRPZ. The DP is the simplest and most illustrative metric, measuring the percentage of correctness denoted properly by the models while predicting the GWRPZ. Therefore, this function holistically represents the entire model's correctness of performance for the predictability. The OQP is a measure of the absolute quality of the predictive model. Therefore, it is a combined aspect of all the measures which summarize the model performance cumulatively. The true positive, false positive and false negative were calculated by comparing the modelled output with respect to the actual groundwater fluctuation scenario of pre and post-monsoon seasons (Fig. 4).

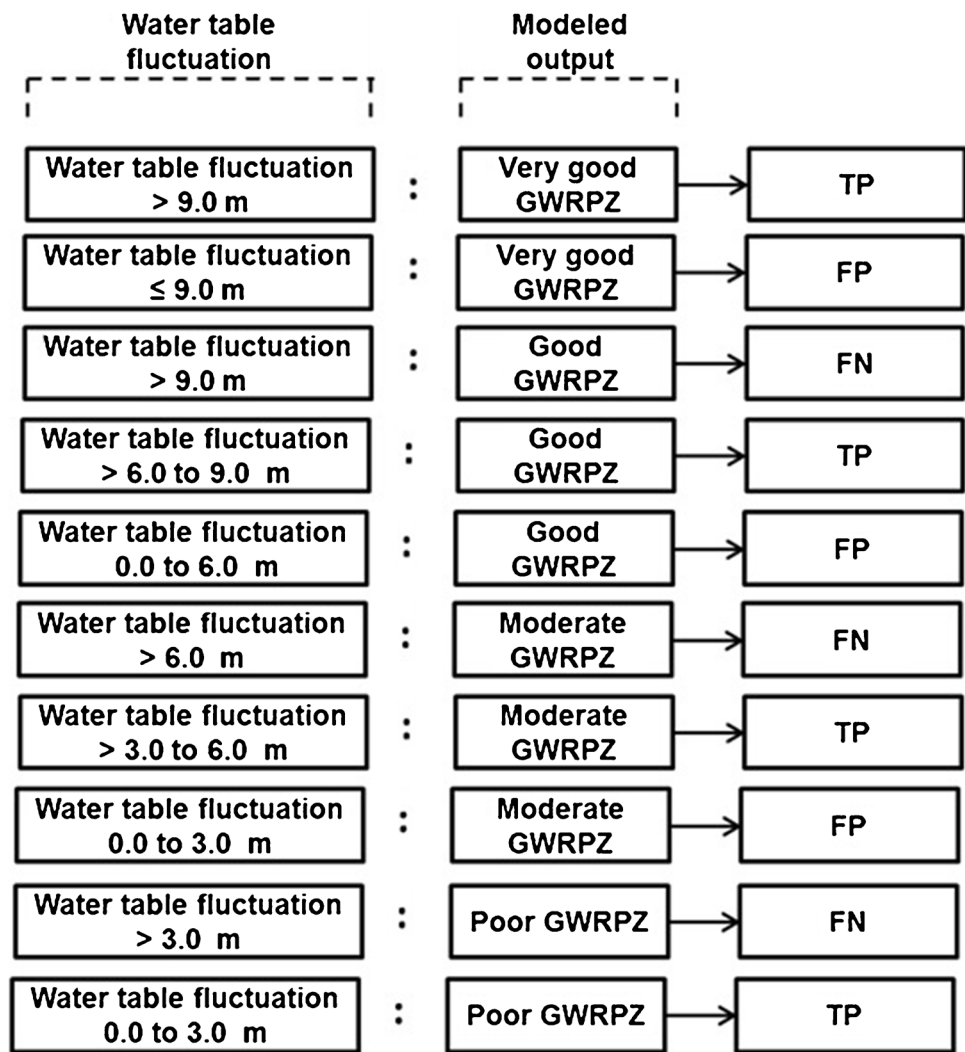
Results

Hydrological thematic layers of parts of the Manjeera basin

Geomorphology

Geomorphology significantly controls the groundwater occurrence, movement, storage and recharge of any hydro-geological province (Kumar and Krishna 2018; Etikala et al. 2019). This study area represents diverse geomorphologic conditions of plateaus along with other associated landforms (Fig. 5a). The types of landforms present within the study area are namely plateau moderately dissected (PLM), plateau slightly dissected (PLS), plateau undissected (PLU) and plateau weathered (PLW). The other dominant landforms are lateritic plain with shallow basement depth (LPSB) (0 to 3 m), moderate basement depth (LPMB) (> 3 to 6 m), deep basement depth (LPDB) (> 6 m), lateritic plain weathered (LPW), valley fill (VF), fractured valley (FVL), butte (B), mesa (MS) and escarpment slope (ES). The FVL and VF with higher chances of groundwater percolation and storage were assigned higher ranks. The LPW, with weathering characteristics along with higher percolation, was assigned a higher rank amongst the other lateritic plain, followed by LPDB, LPMB and LPSB. The greater the depth of the basement, the higher the probability of water percolation and storage. In plateaus, the higher ranks were assigned to PLW, followed by PLU, PLS and PLM. PLW with weathering characteristics demonstrates higher percolation, whereas PLU, PLS and PLM show progressively lower percolation

Fig. 4 A schematic illustration showing the calculation of TP, FP and FN used in the accuracy assessment of AHP and MIF



Water table fluctuation > 9.0 m is indicator for very good GWRPZ; >6.0 to 9.0 m is indicator for good GWRPZ; >3.0 to 6.0 m is indicator for moderate GWRPZ; and 0.0 to 3.0 m is indicator for poor GWRPZ

TP = True positive ; FP = False positive ; FN = False negative

and storage. The MS, B and ES with very less probability of groundwater storage and percolation hence assigned the lower ranks. The details of geomorphology thematic layer AHP and MIF weight and corresponding classes rank are provided in Table 4.

Lineament density (LD)

Lineaments are the surficial manifestation of the sub-surficial lithological characteristics and structural features/weak zones like joints, faults and fractures (O’leary et al. 1976). These lineaments play an important role in

combination with lithology, geomorphology and other associated hydrogeological features towards GWR. Lineaments are conduits for favourable groundwater movement and storage and act as an intensified zone of secondary porosity and permeability (Sreedevi et al. 2005). Lineaments were used for LD map preparation and classification. LD represents the lineament lengths with respect to the area considered (Eq. 16) (Edet and Okereke 1997). LD was expressed in terms of km/km².

$$LD = \sum_{i=1}^n \frac{L_i}{A} \left(\frac{Km}{Km^2} \right) \tag{16}$$

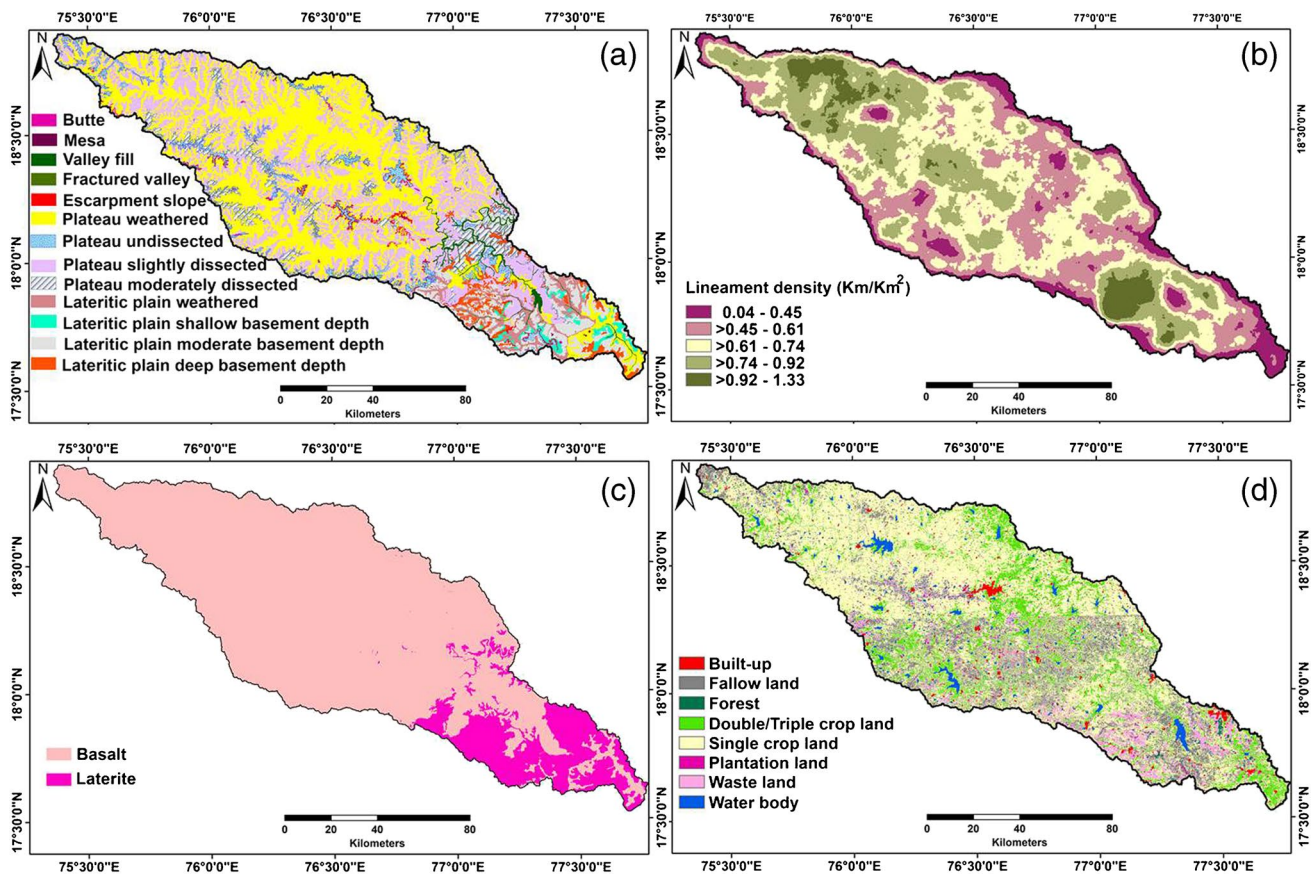


Fig. 5 Controlling hydrogeological thematic layers for groundwater potential. **a** Geomorphology. **b** Lineament density. **c** Lithology. **d** Landuse

where LD is the lineament density; L_i is the total length of lineament in km; and A is the area of the grid in km^2 used in LD computation.

The lineaments of the study area show three distinct alignments in N-S, E-W and NE-SW directions. The range of LD is 0.04 to 1.33 km/km^2 . LD was classified into 5 classes as per natural break of LD values, namely 0.04 to 0.45 km/km^2 , > 0.45 to 0.61 km/km^2 , > 0.61 to 0.74 km/km^2 , > 0.74 to 0.92 km/km^2 and > 0.92 to 1.33 km/km^2 (Fig. 5b). The higher the LD , the greater the chances of water percolation, movement, storage and occurrence (Chaudhry et al. 2019). Therefore, keeping this in mind, the ranks were assigned to LD classes (Table 4). The higher ranking was assigned to greater LD values, and the lower ranking to lesser LD values.

Lithology

Lithology and its variations play a significant part in GWR, relying on the resistance of lithology towards weathering and other denudational characteristics (Kumar et al. 2021). The present study area consists of basalt and laterite (Fig. 5c).

Laterite is the altered production of the host basaltic formation and was formed due to humid tropical weathering. Laterite exhibits hollow and vesicular form leading to favourability towards GWR. Basaltic rock displays noticeably less GWR favourability than the laterites, based on their properties of texture, porosity, permeability, transmissivity and degree of weathering. As basalts bear fewer voids between grains of rock, this leads to water percolation obstruction. Depending on the favourability of GWR, different ranks were assigned (Table 4).

Landuse

Landuse is also a very important factor for GWR and groundwater resource management (Avtar et al. 2010; Sahoo et al. 2017). The landuse classes present within the study area, namely water body, double/triple cropland, single cropland, forest land, plantation land, fallow land, wasteland and built-up area (Fig. 5d). Built-up area represents reducing the impact on GWR with lowest groundwater percolation potential; therefore, lowest rank was assigned. At the same time, the water body demonstrates a higher level of groundwater

Table 4 Assigned rank of different classes associated with thematic layers, computed weight of AHP and MIF

Themes	Classes	Rank	AHP weight	MIF weight
Geomorphology	Escarpment slope	1	0.33	0.19
	Butte/Mesa	2		
	Plateau moderately dissected	3		
	Plateau slightly dissected/lateritic plain shallow basement depth	4		
	Plateau undissected/lateritic plain moderate basement depth	5		
	Plateau weathered/lateritic plain deep basement depth	6		
	Lateritic plain weathered	7		
	Valley fill	8		
	Fractured valley	9		
Lineament density	0.04 to 0.45 km/km ²	1	0.23	0.15
	> 0.45 to 0.61 km/km ²	3		
	> 0.61 to 0.74 km/km ²	5		
	> 0.74 to 0.92 km/km ²	7		
	> 0.92 to 1.33 km/km ²	9		
Lithology	Basalt	5	0.16	0.19
	Laterite	7		
Landuse	Built-up area	2	0.11	0.15
	Wasteland	3		
	Fallow land	4		
	Plantation land	5		
	Forest land	6		
	Single cropland	7		
	Double/triple cropland	8		
	Waterbody	9		
Slope	0 to 2°	9	0.07	0.11
	> 2 to 5°	7		
	> 5 to 10°	5		
	> 10 to 15°	3		
	> 15°	1		
Soil texture	Clay soil	2	0.05	0.06
	Clay skeletal soil	3		
	Loamy soil	5		
	Loamy skeletal soil	6		
Drainage density	0.15 to 0.84 km/km ²	8	0.03	0.09
	> 0.84 to 1.21 km/km ²	6		
	> 1.21 to 1.47 km/km ²	4		
	> 1.47 to 1.77 km/km ²	2		
	> 1.77 to 2.52 km/km ²	1		
Rainfall	715 to 766 mm	2	0.02	0.06
	> 766 to 799 mm	4		
	> 799 to 828 mm	6		
	> 828 to 855 mm	7		
	> 855 to 897 mm	8		

percolation. Hence, highest rank was assigned, followed by double/triple cropland, single cropland, forest land, plantation land, fallow land and wasteland. The details of landuse thematic layer AHP and MIF weight and corresponding classes rank are provided in Table 4.

Slope

Slope controls the surface runoff, thus, influencing the GWR with reference to the residence time of surface water, to infiltrate underground (Arulbalaji et al. 2019). The slopes of the

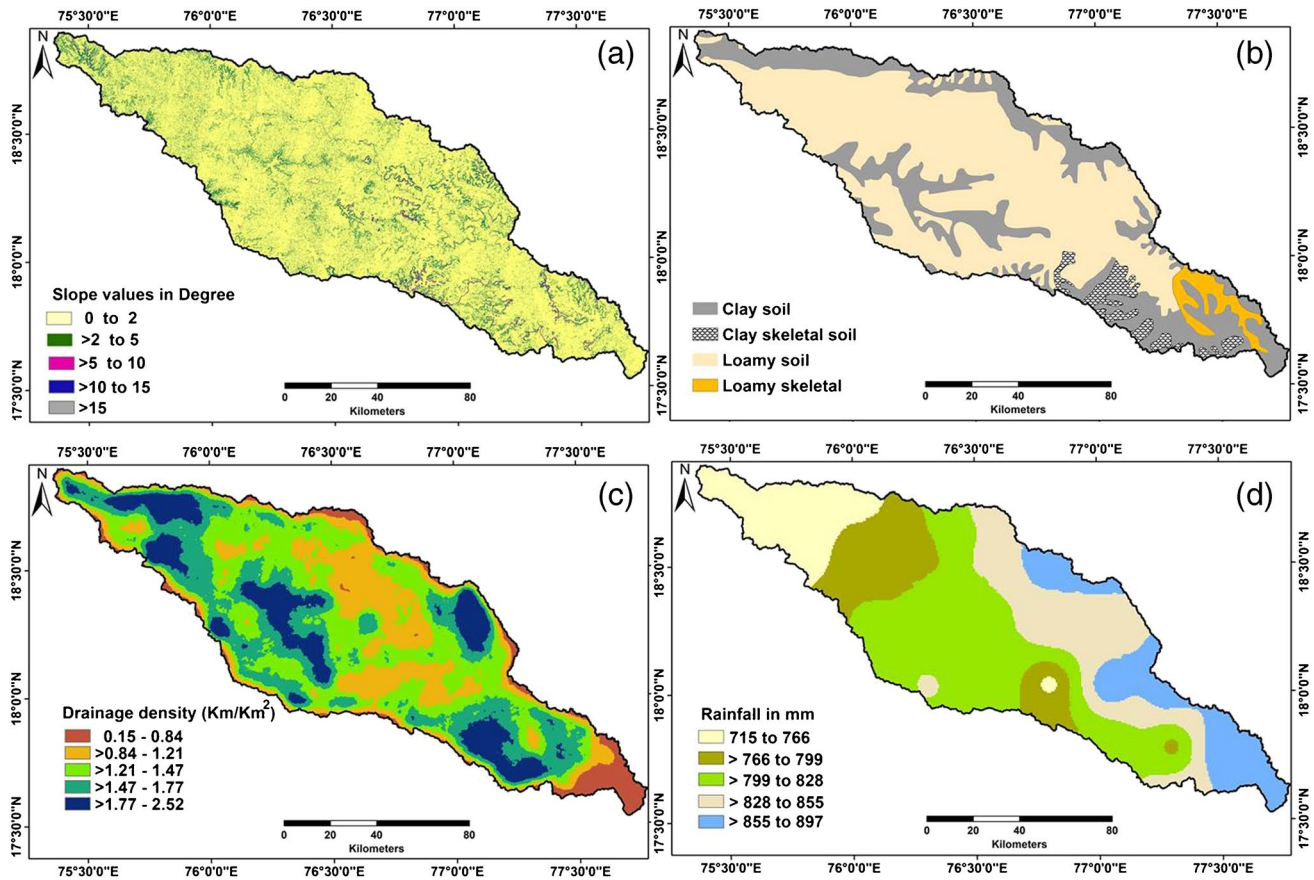


Fig. 6 Controlling hydrogeological thematic layers for groundwater potential. **a** Slope. **b** Soil texture. **c** Drainage density. **d** Rainfall

study area were divided into 5 different classes, namely 0 to 2° as flat terrain > 2 to 5° nearly flat terrain, > 5 to 10° as gently dipping terrain, > 10 to 15° moderately dipping terrain and > 15° highly dipping terrain (Fig. 6a). The flat to nearly flat terrains are good for GWR, rather than moderate to highly dipping regions. Accordingly, the ranks were assigned to different classes of slope (Table 4).

Soil texture

Soil texture is one of the factors controlling surface runoff and the rate of surface water infiltration, which consecutively controls the GWR of the region (Kumar and Krishna 2018). A total of four types of soil texture are present in this study area, namely clay soil, clay skeletal soil, loamy soil and loamy skeletal soil (Fig. 6b). Loamy skeletal soil is best for GWR, which poses the highest rate of water infiltration, with a higher percentage of sand or similar coarser fraction and greater interconnected pore spaces. Clay soil is the worst, with the lowest

rate of water infiltration due to high clay percentage and very low interconnected pore spaces. However, the study area is majorly covered by loamy soil, which is good for GWR, followed by clay skeletal soil, which is comparatively better than clay soil (Table 4).

Drainage density (DD)

The drainage of any province is the resultant product of slope, lithology, geomorphology, rainfall and its absorption nature by soil along with infiltration characteristics (Singha et al. 2019). DD represents the total cumulative length of drainage per unit area (Eq. 17).

$$DD = \sum_{i=1}^n \frac{D_i}{A} \left(\frac{Km}{Km^2} \right) \quad (17)$$

where DD is drainage density; D_i is the total length of drainage in km; and A is the area of the grid in km^2 used in DD computation.

DD describes the competence of the drainage to carry the water of a particular area. The main flow direction of

the study area is towards ESE. The range of DD is 0.15 to 2.52 km/km². DD was classified into 5 classes as per the natural break of DD values, 0.15 to 0.84 km/km², > 0.84 to 1.21 km/km², > 1.21 to 1.47 km/km², > 1.47 to 1.77 km/km² and > 1.77 to 2.52 km/km² (Fig. 6c). DD is inversely proportional to permeability. Therefore, the more the DD, the greater the chance of surface runoff and the less the opportunity towards GWR (Kumar and Krishna 2018). Accordingly, the ranks were assigned to DD classes (Table 4).

Rainfall

Rainfall governs the quantity of water available for percolation underground towards GWR. This study area’s average rainfall ranges between 715 and 897 mm. The rainfall map was

created using IDW spatial interpolation technique for the study area (Fig. 6d). It is classified into five classes, namely 715 to 766 mm, > 766 to 799 mm, > 799 to 828 mm, > 828 to 855 mm and > 855 to 897 mm. The greater the rainfall quantity in any province, the higher the chances of GWR (Singha et al. 2019). Depending upon this concept, higher rainfall-receiving zone are assigned higher ranks and vice versa (Table 4).

Groundwater recharge potential zone map and index by AHP

The delineation of GWRPZ and GWRPZI was accomplished by AHP depending upon the computed weights of the eight thematic layers along with their corresponding class ranks (Table 4) and expressed by Eq. 18.18.

$$GWRPZI = (0.33 * GM_{rk} + 0.23 * LD_{rk} + 0.16 * LT_{rk} + 0.11 * LU_{rk} + 0.07 * SL_{rk} + 0.05 * ST_{rk} + 0.03 * DD_{rk} + 0.02 * RF_{rk}) \tag{18}$$

Figure 7 demonstrates the GWRPZ map and spatial distribution of 4 GWRPZ, namely very good, good, moderate and poor, classified based on natural breaks GWRPZI (ranging from 2.05 to 8.10). Very good GWRPZ covers around 21% (2893 km²) (Fig. 8) of the total study area and mostly coincides with PLW, VF, FVL, LPW and LPDB. This is mainly contributed by the presence of a considerable level of overburden material thickness in combination with a high to a very high level of LD (> 0.74 to 1.33 km/

km²) with flat terrain. The very good GWRPZ is mostly present in NW, SE and some parts of the central region of the study area. The good GWRPZ is covering around 32% (4530 km²) and coinciding with PLS, PLW and LPMB geomorphic landforms along with single cropland as well as moderate to high LD (> 0.61 to 0.92 km/km²). The moderate GWRPZ covers around 32% (4532 km²) and is scattered throughout the study area. This area is mostly characterized by PLU and PLS along with moderate to low

Fig. 7 Controlling hydro-geological thematic layers for groundwater potential

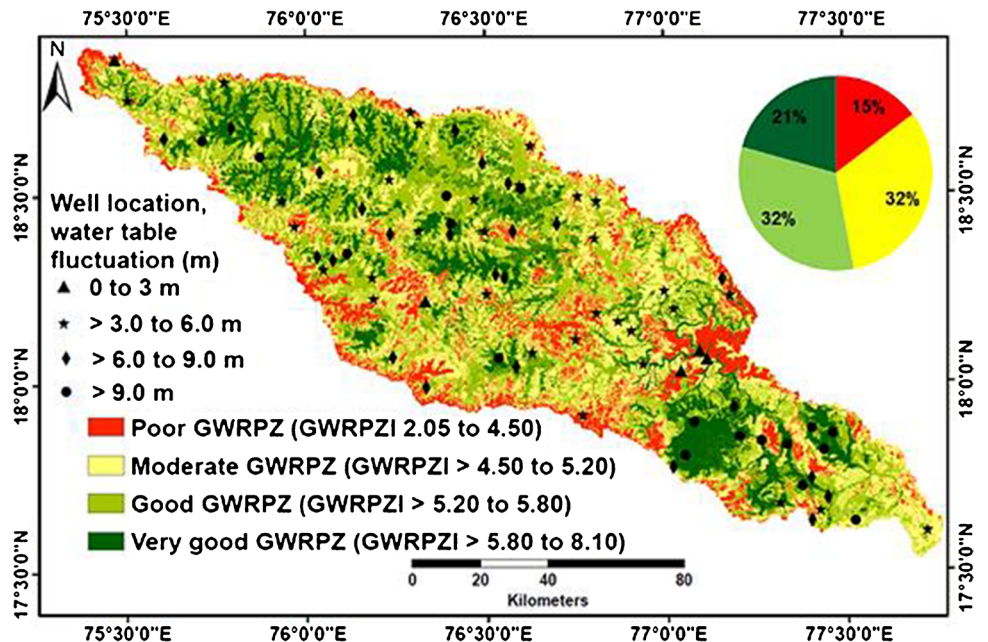
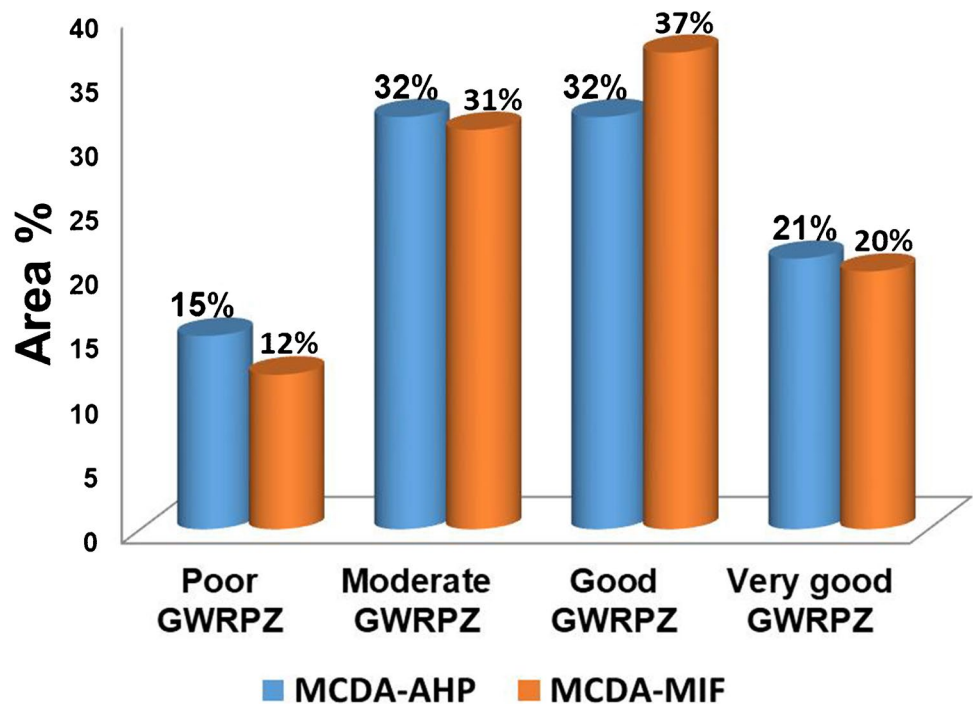


Fig. 8 Spatial distribution of different GWRPZ classes obtained using AHP and MIF for the study area



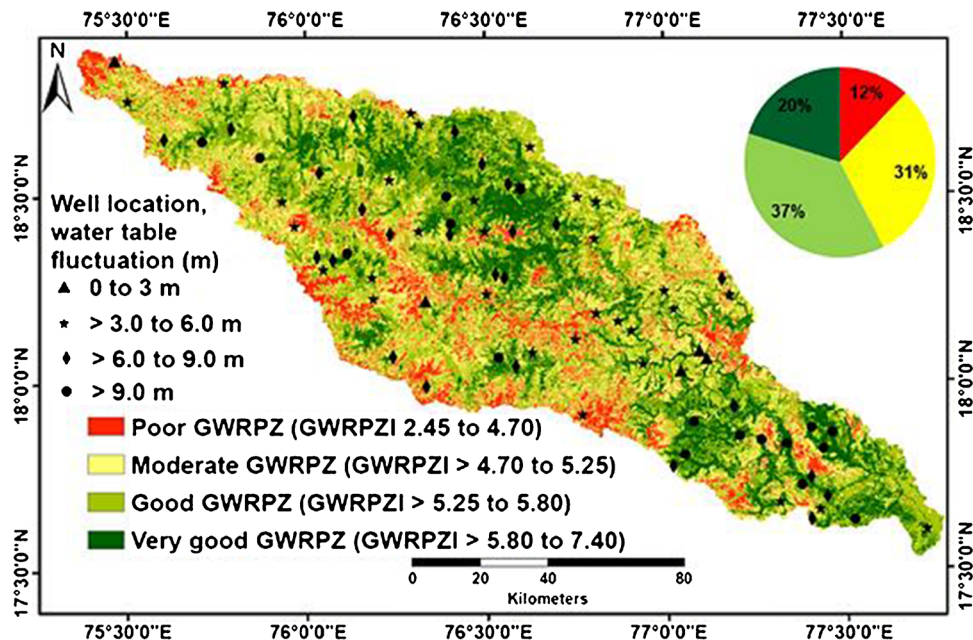
LD (> 0.45 to 0.74 km/km²) and a few wasteland regions. The poor GWRPZ accounts for 15% (2055 km²) of the study area, characterized by PLM, ES, B and MS geomorphic feature along with very low LD (0.04 to 0.45 km/km²), moderate to high slope and mostly coinciding with the built-up area, fallow land, wasteland, except with the wasteland of SE.

Groundwater recharge potential zone map and index by MIF

MIF was conducted for the delineation of the GWRPZ map, based on the calculated weights of the different thematic layers along with their associated classes' assigned ranks (Table 4) and represented by the following Eq. 19.

$$GWRPZI = (0.19 * GM_{rk} + 0.15 * LD_{rk} + 0.19 * LT_{rk} + 0.15 * LU_{rk} + 0.11 * SL_{rk} + 0.06 * ST_{rk} + 0.09 * DD_{rk} + 0.06 * RF_{rk}) \tag{19}$$

Fig. 9 Groundwater recharge potential zone map and index, produced using MIF along with water level fluctuation well locations for accuracy assessment



GWRPZ was classified into 4 distinct zones as per the GWRPZI (ranging from 2.45 to 7.40) natural breaks, namely very good, good, moderate and poor (Fig. 9). The very good GWRPZ covers around 20% (2820 km²) of the study area mostly in the north-central and SE portion of the study area (Figs. 8 and 9). This area is mainly coinciding with PLW, VF, FVL, LPW and LPDB geomorphic features along with cropland (double/triple cropland and single cropland) and flat terrain. The good GWRPZ covers around 37% (5237 km²) and coinciding PLS and PLW geomorphic feature along with single cropland. The moderate GWRPZ covers around 31% (4264 km²) of the study area coinciding with moderate to low LD (> 0.45 to 0.74 km/km²). This zone is mostly scattered and distributed throughout the study area. The poor GWRPZ is characterized by built-up area, fallow land along with B, MS and ES geomorphic landforms along with very low LD (0.04 to 0.45 km/km²). This zone covers around 12% of the study area accounting for 1689 km².

Sensitivity analysis results

Map removal sensitivity analysis (MRSA) The MRSA for AHP and MIF were conducted by removing different thematic layers, each one at one instance and using the remaining thematic layers to generate a new GWRPZ map. In the case of AHP, high sensitivity (mean MRSA_i = 2.69) was observed with the removal of the geomorphology layer, as the geomorphology thematic layer was assigned the highest weight. Moderate sensitivity was observed in the case of DD, rainfall, LD and soil texture (mean MRSA_i = 1.48, 1.47, 1.37 and 1.23, respectively). Low sensitivity was observed for lithology, landuse and slope (mean MRSA_i = 0.55, 0.43 and 0.39, respectively). In the case of MIF, high sensitivity was observed in the soil texture thematic layer (mean MRSA_i = 1.14); moderate sensitivity value was observed in DD, lithology, rainfall and landuse (mean MRSA_i 0.99, 0.91, 0.88 and 0.86 respectively). Lower sensitivity is represented by geomorphology, LD and slope (mean MRSA_i 0.77, 0.68 and 0.49, respectively). The results (Table S1) clearly represent that the MRSA_i depends not only on that single thematic layer weight and its associated class ranks but also on other thematic layer weights and ranks along with their spatial distribution and variability.

Single parameter sensitivity analysis (SPSA) SPSA was performed for a better understanding of thematic layer effective weight towards the formulation of the GWRPZ map. The result for both AHP and MIF shows effective weight in comparison with the assigned weight, with very less deviation. This also reveals which thematic layer is most impactful (Table S2). In the case of AHP, the highest effective weight is shown by geomorphology (mean SPSA_i = 31.25), followed by LD, lithology, landuse, slope, soil texture, DD and

rainfall (mean SPSA_i values are 20.60, 16.37, 13.36, 10.08, 3.91, 2.23 and 2.21 respectively). Therefore, the effective weight is in line with the assigned weight and following the same hierarchy. In the case of MIF, the highest effective weight is shown by lithology (mean SPSA_i = 18.85), followed by landuse, geomorphology, slope, LD, rainfall, DD and soil texture (mean SPSA_i values are 17.64, 17.59, 15.33, 13.34, 6.37, 6.34 and 4.55 respectively). Therefore, the effective weight and assigned weight are close to each other and inline.

Accuracy assessment of the results The feasibility of GWR based on the GWRPZ map is only achievable if the GWRPZ map delineated by AHP and MIF is getting validated with the groundwater fluctuation data of the reference observatory wells (Ghosh et al. 2020; Kumar et al. 2021). Therefore, an accuracy assessment was carried out to assess the effectiveness of this research. Therefore, a total of 79 observation wells of pre and post-monsoon (2017) water level fluctuation data (Figs. 7 and 9) of Central Ground Water Board (CGWB), Karnataka State Groundwater Department and Groundwater Surveys & Development Agency (GSDA)-Maharashtra, were used. The groundwater fluctuation level shows four distinct levels of fluctuation classes, and the threshold of those classes was rounded to a near integer value. The higher the level of fluctuation, the greater will be the water resource dynamicity; hence, the greater will be the groundwater storage and recharge potential (Chowdhury et al. 2010; Charan et al. 2020). The four classes are namely very good (fluctuation > 9.0 m), good (> 6.0 to 9.0 m), moderate (> 3.0 to 6.0 m) and poor (0 to 3.0 m).

Figure 7 AHP-derived GWRPZ map demonstrated that 4 wells coincided with poor GWRPZ and all of which are with water table fluctuation of ≤ 3 m. A total of 32 wells coincided with moderate GWRPZ, out of which 28 are with fluctuation > 3.0 to 6.0 m, 1 well is ≤ 3 m and 3 wells are with fluctuation > 6 m. Similarly, out of the total 26 wells that fell in good GWRPZ, 4 wells are with ≤ 6 m fluctuation, 18 wells are with fluctuation > 6 m to ≤ 9 m and 4 wells demonstrated fluctuation of > 9 m. Moreover, out of the total 17 wells that coincided with a very good GWRPZ, a total of 12 are with water table fluctuation > 9 m, and 5 wells are with fluctuation ≤ 9 m. Therefore, the two computed potential error BF and MF is 0.16 and 0.11, respectively, which is very less. The DP is 89.86%, whereas the OQP represents a good result, i.e. 78.48% (Table S3)

Figure 9 MIF-derived GWRPZ map demonstrated that 10 wells are fallen on poor GWRPZ, out of which 4 match with the ground observation, i.e. water table fluctuation within 3 m, others are with fluctuation > 3 m. Moderate GWRPZ coincided with 31 wells, out of which 23 wells have fluctuation > 3 to ≤ 6 m, 1 well is ≤ 3 m and 7 wells are with fluctuation > 6 m. Similarly, 22 wells coincided with good

GWRPZ, where 16 wells are with fluctuation > 6.0 to 9.0 m, 4 wells are with ≤ 6 m fluctuation and 2 wells demonstrated a fluctuation > 9 m. Furthermore, 16 wells coincided with very good GWRPZ, where 14 wells are with fluctuation > 9 m and 2 wells are with fluctuation ≤ 9 m. Thus, the computed two potential errors BF and MF for this MIF-derived model are very less (BF = 0.12, MF = 0.26). The DP is 79.17% and OQP is 72.15%, which indicates higher accuracy of delineation (Table S3)

All these values of accuracy assessment eventually validate the authenticity and correctness of the research.

Discussion

This section of the article discusses the control of the different hydrogeological thematic variables over GWRPZ, sensitivity and validity.

Lately, there are many noteworthy literatures that investigated the control of different hydrogeological thematic variables in GWR and GWRPZ delineation using geospatial techniques (Dar et al. 2020; Verma et al. 2020; Doke et al. 2021). The research finding of Dar et al. (2020) in the Kashmir Himalayan region of India revealed that groundwater recharge condition is mainly controlled by lithology, geomorphology, slope and landuse. More precisely, excellent GWR conditions are associated with alluvium formation, flat topography and higher porosity permeability, whereas the low potential of recharge regions are located in high hilly regions with steep slopes, denudation hills/ridges with high DD. Similarly, the research of Verma et al. (2020) in Lucknow, Uttar Pradesh, India, also demonstrated the control of geomorphic features such as ox-bow lakes and palaeochannels in excellent GWRPZ. The research findings of Doke et al. (2021) of basaltic terrain in western Maharashtra, India, represented the influence of runoff, landuse, slope, rainfall and distance of river/lineaments in GWR. However, in this present research, GWR potentiality at its highest is governed by geomorphology and LD, followed by lithology and landuse. The other four variables slope, soil texture, DD and rainfall control are less. Geomorphic land forms FVL, VF, LPW show a higher probability of groundwater percolation and storage. LPDB, LPMB and LPSB show regressive GWR conditions, respectively, depending upon the depth of the basement, which boosts the probability of water percolation and storage. Similarly, PLM, PLS, PLU and PLW display progressive characteristics of percolation. The MS, B and ES exhibit significantly less probability of groundwater storage and percolation. LD is directly proportional to GWR. LD is comparatively very high towards NW and SE of the study area, whereas the central region exhibits high, moderate and low LD comparatively. Therefore, these

higher LD zones always indicate greater chances of GWR. Laterite shows more probability of GWR due to its vesicular and hollow nature. The built-up area demonstrates low to nil impact on GWR. In contrast, the water body represents the possibility of more excellent groundwater percolation regressively followed by double/triple cropland, single cropland, forestland, plantation land, fallow land and wasteland. The study area primarily represents flat to nearly flat terrain, which is suitable for GWR, rather than moderate to high dipping region, as slope controls the surface runoff, which influences GWR inversely. Loamy skeletal soil with a higher percentage of sand or a similar coarser fraction and greater interconnected pore spaces demonstrates a higher probability of water infiltration. Clay soil shows a low to nil probability of GWR with high clay percentage and very low interconnected pore spaces. Moreover, skeletal texture increases the GWR capabilities. Therefore, clay skeletal soil is better than clay soil. DD demonstrates an inverse relationship with GWR, as it is a measure of the competency of surface runoff. The more significant the surface runoff, the lesser the GWR. The main flow direction of the study area is towards ESE. DD is comparatively very high towards NW, SE, ESE and the west-central portion of the study area. This study witnessed higher rainfall in the eastern region compared to the western side. Therefore, GWR is more suitable towards the east portion of the study area.

The purpose of GWRPZ in any province is to develop a sustainable scenario of groundwater condition (Abijith et al. 2020; Aju et al. 2021). Previous researchers showcased the utility of MCDA-driven AHP and MIF model capabilities in GWR and are found to be very popular for groundwater sustainability in similar and different hydrogeological provinces (Dar et al. 2020; Verma et al. 2020; Doke et al. 2021). In this research, the AHP model-derived very good GWRPZ is mainly controlled by the geomorphic landforms such as PLW, VF, FVL, LPW and LPDB. The presence of a considerable level of overburdened material in combination with high to very high levels of LD, as well as flat terrain, also plays a significant role in forming excellent recharge potential. This zone is primarily observed in NW, SE and some parts of the central region of the study area. Landforms such as PLS, PLW and LPMB combined with single-crop agricultural land and moderate to high LD control the GWR characteristics of good GWRPZ. These hydrogeological variables hold positive control over good recharge potential. On the other hand, moderate GWRPZ is scattered chiefly and governed by the presence of PLU and PLS in combination with wastelands and medium to low LD, which usually demonstrates moderate recharge potential. PLM, ES, B and MS geomorphic landforms along with very low LD, medium to high slope and mostly coinciding with the built-up area, fallow land and wasteland were associated with nil to limited recharge potential, which governs the GWR condition of poor GWRPZ.

MIF-calculated very good GWRPZ are primarily in the north-central and SE portion. This area GWR condition is mainly governed by the high positive influence of PLW, VF, FVL, LPW and LPDB geomorphic landforms along with cropland (double/triple cropland and single cropland) and flat terrain. The good GWRPZ is controlled by the positive impact of PLS and PLW geomorphic features along with single cropland. The moderate GWRPZ is mainly scattered and regulated by the moderate to low LD, which demonstrates the intermediate/average potential of recharge. Built-up area, fallow land B, MS, ES geomorphic landforms and very low LD with negative influence govern the GWR potential of poor GWRPZ with a very limited to nil recharge potential.

In this research on GWRPZ, both the MCDA models AHP and MIF demonstrated efficient GWRPZ. The accuracy assessment results with less potential error represented by BF and MF, along with high precision of delineation for GWRPZ demonstrated by DP and OQP, validate this research outputs. This efficiency was achieved based on methods of the model's multicriteria decision with consistency over the judgement. Moreover, these models very effectively interacted between the hydrogeological controlling variables towards the delineation of GWRPZ. These MCDA models, in combination with geospatial techniques, demonstrated their potency while delineating GWRPZ in this critical hydrogeological province.

Sensitivity analysis MRSA results demonstrate a few crucial findings that the impact of each thematic layer depends not only on that single thematic layer weight and its associated class ranks but also on other thematic layer weights and ranks, their interrelationship and their spatial distribution and variability. While SPSA result for both AHP and MIF shows effective weight compared to the assigned weight, with significantly less deviation. These also reveal which thematic layer is most impactful. The results of the SPSA indicate that the effective weights are in line with assigned weights and follow the same hierarchy for the hydrological thematic variables.

Conclusion

In water security management, groundwater recharge potentiality delineation is one of the fundamental factors. This study aims to investigate the effectiveness of two MCDA methods, AHP and MIF, to overcome the obstacle of hydrogeological complexity of the Deccan plateau towards precise delineation of GWRPZ. The AHP computed GWRPZI and classified the GWRPZ as very good, good, moderate and poor zones accounting for 21%, 32%, 32% and 15% of the study area, respectively. In contrast, the MIF accounts for a very good 20%, good 37%, moderate 31% and poor 12% GWRPZ, respectively. Geomorphology, LD, lithology and landuse mainly control the recharge

potentiality. In detail, it is the combined and coupled effect of depositional and denudational characteristics of geomorphic landforms in combination with lithological properties and secondary porosity-driven factors such as LD as well as the landuse. The other hydrogeological variables like slope, soil texture, DD and rainfall effects are less compared to geomorphology, LD, lithology and landuse. Sensitivity analysis demonstrated how each thematic layers weights and ranks along with spatial variability, distribution along with different themes interrelationship controls, and signifies the GWRPZ. It also revealed that the assigned weight for both the models is in line with the effective weight and with very less deviation from the actual. This analysis further revealed GWRPZ control is very specifically related to its hydrogeological settings in combination with different thematic variable interrelationships. The accuracy assessment result demonstrates a very good OQP for both the models (AHP = 78.48% and MIF = 72.15%), with very good DP (AHP = 89.86% and MIF = 79.17%) and less induced errors. Thus, this research applicability can provide a deep insight into a realistic evaluation of groundwater sustainability in this and similar hydrogeological provinces. Therefore, based on the scientific output and objective, this GWRPZ map can assist the planners/policymakers/local administration in accurate groundwater abstraction, development and recharge strategies. Still, it is very necessary for any site-specific groundwater recharge strategies, and the scale of interpretation and analysis is very important.

Supplementary Information The online version contains supplementary material available at <https://doi.org/10.1007/s12517-023-11323-2>.

Acknowledgements The authors wish to express their sincere thanks to Dr. Prakash Chauhan, Director, NRSC, Dr. V. V. Rao, Deputy Director, RSA NRSC and colleagues of Geosciences and of NRSC, for their encouragement and help to carry out this study.

Data availability Data is available on reasonable request, as per organizational policy and privacy/ethical restrictions.

Declarations

Competing interests The authors declare no competing interests.

References

- Abijith D, Saravanan S, Singh L, Jennifer JJ, Saranya T, Parthasarathy KSS (2020) GIS-based multicriteria analysis for identification of potential groundwater recharge zones—a case study from Ponnaniyaru watershed, Tamil Nadu, India. *HydroRes* 3:1–14. <https://doi.org/10.1016/j.hydres.2020.02.002>
- Agarwal R, Garg PK (2016) Remote sensing and GIS based groundwater potential & recharge zones mapping using multicriteria decision making technique. *Water Resour Manag* 30(1):243–260. <https://doi.org/10.1007/s11269-015-1159-8>
- Aju CD, Achu AL, Raicy MC, Reghunath R (2021) Identification of suitable sites and structures for artificial groundwater recharge for

- sustainable water resources management in Vamanapuram River Basin, South India. *HydroRes* 4:24–37. <https://doi.org/10.1016/j.hydres.2021.04.001>
- Andualem TG, Demeke GG (2019) Groundwater potential assessment using GIS and remote sensing: a case study of Guna tana landscape, upper blue Nile Basin. Ethiopia. *J Hydrol Reg Stud* 24:100610. <https://doi.org/10.1016/j.ejrh.2019.100610>
- Arulbalaji P, Padmalal D, Sreelash K (2019) GIS and AHP techniques based delineation of groundwater potential zones: a case study from southern Western Ghats. *India Sci Rep* 9(1):1–17. <https://doi.org/10.1038/s41598-019-38567-x>
- Avtar R, Singh CK, Shashtri S, Singh A, Mukherjee S (2010) Identification and analysis of groundwater potential zones in Ken-Betwa river linking area using remote sensing and geographic information system. *Geocarto Int* 25(5):379–396. <https://doi.org/10.1080/10106041003731318>
- Bali BA, Kumawat BL, Singh AJ, Chopra RA (2015) Evaluation of ground water in Sriganganagar district of Rajasthan. *The Ecoscan* 9(1&2):133–136
- Bennia A, Srivastav SK, Chatterjee RS (2013) Groundwater investigations using optical and microwave remote sensing data in Solani Watershed, India. In: Margottini C, Canuti P, Sassa K (eds) *Landslide Science and Practice*. Springer, Berlin, pp 95–100. https://doi.org/10.1007/978-3-642-31445-2_12
- Bhattacharya RK, Chatterjee ND, Das K (2020) An integrated GIS approach to analyze the impact of land use change and land cover alteration on ground water potential level: a study in Kangsabati Basin, India. *Groundw Sustain Dev* 11:100399. <https://doi.org/10.1016/j.gsd.2020.100399>
- Bogardi JJ, Dudgeon D, Lawford R, Flinkerbusch E, Meyn A, Pahl-Wostl C, Vielhauer K, Vörösmarty C (2012) Water security for a planet under pressure: interconnected challenges of a changing world call for sustainable solutions. *Curr Opin Environ Sustain* 4(1):35–43. <https://doi.org/10.1016/j.cosust.2011.12.002>
- Census (2011) Census of India 2011. www.censusindia.gov.in/2011. Accessed 2 Apr 2022
- Central Ground Water Board (2012) Ground water information booklet Bidar district, Karnataka, SouthWestern Region, Bangalore, India. https://cgwb.gov.in/District_Profile/karnataka/2012/BIDAR_brochure%202012.pdf
- Central Ground Water Board (2013) Ground Water information Latur district, Maharashtra Central region, Nagpur, India. https://cgwb.gov.in/District_Profile/Maharashtra/Latur.pdf
- Central Ground Water Board (2017a) Report on dynamic ground water resources of India, New Delhi. <http://cgwb.gov.in/GW-Assessment/GWRA-2017-National-Compilation.pdf>
- Central Ground Water Board (2020 and 2021) Groundwater year book of Maharashtra and Union territory of Dara and Nagar Haveli, Nagapur. https://cgwb.gov.in/Regions/CR/Reports/GW%20Year%20book%202020_2021_CR_Nagpur_Maharashtra.pdf
- Central Ground Water Board (2014) Ground water information Beed district, Maharashtra Central region, Nagpur, India. https://cgwb.gov.in/District_Profile/Maharashtra/Beed.pdf
- Central Ground Water Board (2017b) Ground Water year book of Karnataka, South Western Region, Bangalore, India. https://cgwb.gov.in/Regions/SWR/Reports/Karnataka_2016-17.pdf
- Charan VS, Jyothi BN, Saha R, Wankhede T, Das IC, Venkatesh J (2020) An integrated geohydrology and geomorphology based subsurface solid modelling for site suitability of artificial groundwater recharge: Bhalki micro-watershed, Karnataka. *J Geol Soc India* 96(5):458–466. <https://doi.org/10.1007/s12594-020-1583-0>
- Chaudhry AK, Kumar K, Alam MA (2021) Mapping of groundwater potential zones using the fuzzy analytic hierarchy process and geospatial technique. *Geocarto Int* 36(20):2323–2344. <https://doi.org/10.1080/10106049.2019.1695959>
- Chen Y, Chen W, Chandra Pal S, Saha A, Chowdhuri I, Adeli B, Janizadeh S, Dineva AA, Wang X, Mosavi A (2021) Evaluation efficiency of hybrid deep learning algorithms with neural network decision tree and boosting methods for predicting groundwater potential. *Geocarto Int* 37(19):5564–84. <https://doi.org/10.1080/10106049.2021.1920635>
- Chowdhury A, Jha MK, Chowdary VM (2010) Delineation of groundwater recharge zones and identification of artificial recharge sites in West Medinipur district, West Bengal, using RS, GIS and MCDM techniques. *Environ Earth Sci* 59(6):1209–1222. <https://doi.org/10.1007/s12665-009-0110-9>
- CWC-Central Water Commission, National Remote Sensing Centre (NRSC) (2014) Watershed atlas of India. 1–214. <https://doi.org/10.13140/RG.2.2.30331.52009>
- Dar T, Rai N, Bhat A (2020) Delineation of potential groundwater recharge zones using analytical hierarchy process (AHP). *Geol Ecol Landsc* 5(4):292–307. <https://doi.org/10.1080/24749508.2020.1726562>
- Das B, Pal SC (2020) Assessment of groundwater vulnerability to over-exploitation using MCDA, AHP, fuzzy logic and novel ensemble models: a case study of Goghat-I and II blocks of West Bengal, India. *Environ Earth Sci* 79(5):1–16. <https://doi.org/10.1007/s12665-020-8843-6>
- Dasgupta S, Mukherjee S (2019) Remote sensing in lineament identification: examples from western India. In: *Developments in structural geology and tectonics*, vol. 5. Elsevier, pp 205–221. <https://doi.org/10.1016/B978-0-12-814048-2.00016-8>
- Dharpure JK, Goswami A, Patel A, Kulkarni AV (2021) Quantification of groundwater recharge and its spatio-temporal variability in the Ganga river basin. *Geocarto Int* 37(18):5376–5399. <https://doi.org/10.1080/10106049.2021.1914748>
- Doke AB, Zolekar RB, Patel H, Das S (2021) Geospatial mapping of groundwater potential zones using multi-criteria decision-making AHP approach in a hardrock basaltic terrain in India. *Ecol Indic* 127:107685. <https://doi.org/10.1016/j.ecolind.2021.107685>
- Edet AE, Okereke CS (1997) Assessment of hydrogeological conditions in basement aquifers of the Precambrian Oban massif, southeastern Nigeria. *J Appl Geophys* 36(4):195–204. [https://doi.org/10.1016/S0926-9851\(96\)00049-3](https://doi.org/10.1016/S0926-9851(96)00049-3)
- Edge TL (2015) Water conflicts across regions and sectors: case study of Latur city. https://www.acccrn.net/sites/default/files/publication/attach/latur_water_crisis_2014_cac_308_05dec2015.pdf
- Eslamian S, Parvizi S, Ostad-Ali-Askari K, Talebmorad H (2018) Water. In: Bobrowsky P, Marker B (eds) *Encyclopedia of engineering geology*. Springer, Cham. https://doi.org/10.1007/978-3-319-12127-7_295-1
- Etikala B, Golla V, Li P, Renati S (2019) Deciphering groundwater potential zones using MIF technique and GIS: a study from Tirupati area, Chittoor District, Andhra Pradesh, India. *HydroRes* 1:1–7. <https://doi.org/10.1016/j.hydres.2019.04.001>
- Gesim NA, Okazaki T (2018) Identification of groundwater artificial recharge sites in Herat city, Afghanistan, using fuzzy logic. *Int J Eng Tech Res* 8(2):40–45
- Ghosh D, Mandal M, Banerjee M, Karmakar M (2020) Impact of hydro-geological environment on availability of groundwater using analytical hierarchy process (AHP) and geospatial techniques: a study from the upper Kangsabati river basin. *Groundw Sustain Dev* 11:100419. <https://doi.org/10.1016/j.gsd.2020.100419>
- GSDA (2012) Report on dynamic ground water resources of Maharashtra (2011–12). Pune: Groundwater Survey and Development Agency, GoM. https://gsda.maharashtra.gov.in/english/admin/PDF_Files/1559974566_Talukawise_GWA2011-12_compressed.pdf
- Guha A, Roy P, Singh S, Kumar KV (2018) Integrated use of LANDSAT 8, ALOS-PALSAR, SRTM DEM and ground GPR

- data in delineating different segments of alluvial fan system in Mahananda and Tista rivers, West Bengal, India. *J Indian Soc Remote Sens* 46(4):501–514. <https://doi.org/10.1007/s12524-017-0711-9>
- Gupta RP (2003) *Remote sensing geology*, 1st edn. Springer, New Delhi, p 650
- Javadi S, Saatsaz M, Shahdany SMH, Neshat A, Milan SG, Akbari S (2021) A new hybrid framework of site selection for groundwater recharge. *Geosci Front* 12(4):101144. <https://doi.org/10.1016/j.gsf.2021.101144>
- Jena S, Panda RK, Ramadas M, Mohanty BP, Pattanaik SK (2020) Delineation of groundwater storage and recharge potential zones using RS-GIS-AHP: application in arable land expansion. *Remote Sens Appl: Soc Environ* 19:100354. <https://doi.org/10.1016/j.rsase.2020.100354>
- Jhariya DC, Khan R, Mondal KC, Kumar T, Singh VK (2021) Assessment of groundwater potential zone using GIS based multi influencing factor (MIF), multicriteria decision analysis (MCDA) and electrical resistivity survey techniques in Raipur city, Chhattisgarh. India. *Aqua Water Infrastruct Ecosyst Soc* 70(3):375–400. <https://doi.org/10.2166/aqua.2021.129>
- Kadam AK, Umrikar BN, Sankhua RN (2020) Assessment of recharge potential zones for groundwater development and management using geospatial and MCDA technologies in semiarid region of Western India. *SN Appl Sci* 2(2):1–11. <https://doi.org/10.1007/s42452-020-2079-7>
- Kaliraj S, Chandrasekar N, Magesh NS (2014) Identification of potential groundwater recharge zones in Vaigai upper basin, Tamil Nadu, using GIS-based analytical hierarchical process (AHP) technique. *Arab J Geosci* 7(4):1385–1401. <https://doi.org/10.1007/s12517-013-0849-x>
- Khan A, Govil H, Taloor AK, Kumar G (2020) Identification of artificial groundwater recharge sites in parts of Yamuna River basin India based on remote sensing and geographical information system. *Groundw Sustain Dev* 11:100415. <https://doi.org/10.1016/j.gsd.2020.100415>
- Kumar A, Krishna AP (2018) Assessment of groundwater potential zones in coal mining impacted hard-rock terrain of India by integrating geospatial and analytic hierarchy process (AHP) approach. *Geocarto Int* 33(2):105–129. <https://doi.org/10.1080/10106049.2016.1232314>
- Kumar A, Pramod Krishna A (2020) Groundwater vulnerability and contamination risk assessment using GIS-based modified DRAS-TIC-LU model in hard rock aquifer system in India. *Geocarto Int* 35(11):1149–1178. <https://doi.org/10.1080/10106049.2018.1557259>
- Kumar T, Gautam AK, Kumar T (2014) Appraising the accuracy of GIS-based multicriteria decision making technique for delineation of groundwater potential zones. *Water Resour Manag* 28(13):4449–4466. <https://doi.org/10.1007/s11269-014-0663-6>
- Kumar M, Singh P, Singh P (2021) Fuzzy AHP based GIS and remote sensing techniques for the groundwater potential zonation for Bundelkhand craton region, India. *Geocarto Int* 37(22):6671–94. <https://doi.org/10.1080/10106049.2021.1946170>
- Lee DS, Shan J, Bethel JS (2003) Class-guided building extraction from Ikonos imagery. *Photogramm Eng Remote Sens* 69(2):143–150. <https://doi.org/10.14358/PERS.69.2.143>
- Lee S, Hong SM, Jung HS (2018) GIS-based groundwater potential mapping using artificial neural network and support vector machine models: the case of Boryeong city in Korea. *Geocarto Int* 33(8):847–861. <https://doi.org/10.1080/10106049.2017.1303091>
- Lodwick WA, Monson W, Svoboda L (1990) Attribute error and sensitivity analysis of map operations in geographical information systems: suitability analysis. *Int J Geogr Inf Syst* 4(4):413–428. <https://doi.org/10.1080/02693799008941556>
- Malczewski J (1999) *GIS and multicriteria decision analysis*. John Wiley and Sons Inc, New York
- Martha TR, Kerle N, Van Westen CJ, Jetten V, Kumar KV (2012a) Object-oriented analysis of multi-temporal panchromatic images for creation of historical landslide inventories. *ISPRS J Photogramm Remote Sens* 67:105–119. <https://doi.org/10.1016/j.isprsjprs.2011.11.004>
- Martha TR, Saha R, Kumar KV (2012b) Synergetic use of satellite image and DEM for identification of landforms in a ridge-valley topography. *Int j Geosci* 3(3):480–489. <https://doi.org/10.4236/ijg.2012.33051>
- Mathai J, Das IC, Subramanian SK, Lenin KS, Dadhwal VK (2015) Coupling geomorphology parameters with lithology for micro-level groundwater resource assessment: a case study from semi-arid hard rock terrain in Tamil Nadu, India. *Arab J Geosci* 8(10):8077–8087. <https://doi.org/10.1007/s12517-015-1839-y>
- Mishra AK, Rawat KS, Ahmed N (2010) Selection of potential sites for augmenting groundwater recharge in Manesar nala watershed in Gurgaon (Haryana) using RS-GIS approach. *Indian J Soil Water Conserv* 9:234–244
- Mohamed MM, Elmahdy SI (2017) Fuzzy logic and multicriteria methods for groundwater potentiality mapping at Al Fo'ah area, the United Arab Emirates (UAE): an integrated approach. *Geocarto Int* 32(10):1120–1138. <https://doi.org/10.1080/10106049.2016.1195884>
- Mseli ZH, Mwegoha WJ, Gaduputi S (2021) Identification of potential groundwater recharge zones at Makutupora basin, Dodoma Tanzania. *Geol Ecol Landsc* 1–14. <https://doi.org/10.1080/24749508.2021.1952763>
- Mukherjee P, Singh CK, Mukherjee S (2012) Delineation of groundwater potential zones in arid region of India—a remote sensing and GIS approach. *Water Resour Manag* 26(9):2643–2672. <https://doi.org/10.1007/s11269-012-0038-9>
- Murmu P, Kumar M, Lal D, Sonker I, Singh SK (2019) Delineation of groundwater potential zones using geospatial techniques and analytical hierarchy process in Dumka district, Jharkhand. India. *Groundw Sustain Dev* 9:100239. <https://doi.org/10.1016/j.gsd.2019.100239>
- Napolitano P, Fabbri AG (1996) Single-parameter sensitivity analysis for aquifer vulnerability assessment using DRASTIC and SINTACS. *IAHS Publ-Series Proc Rep-Intern Assoc Hydrol Sci* 235(235):559–566
- Navane VS, Sahoo SN (2021) Identification of groundwater recharge sites in Latur district of Maharashtra in India based on remote sensing, GIS and multi-criteria decision tools. *Water Environ J* 35(2):544–559. <https://doi.org/10.1111/wej.12650>
- Nithya CN, Srinivas Y, Magesh NS, Kaliraj S (2019) Assessment of groundwater potential zones in Chittar basin, Southern India using GIS based AHP technique. *Remote Sens Appl Soc Environ* 15:100248. <https://doi.org/10.1016/j.rsase.2019.100248>
- NLULC (2007) National land use and land cover mapping using multi-temporal AWiFS data, NRSA/RSGIS-AA/NRC-AWiFS/PROJREP/R01/JUN07. <https://bhuvanapp1.nrsc.gov.in/2dresources/thematic/LULC250/0506.pdf>. Accessed 1 Apr 2022
- Norouzi H, Shahmohammadi-Kalalagh S (2019) Locating groundwater artificial recharge sites using random forest: a case study of Shabestar region, Iran. *Environ Earth Sci* 78(13):1–11. <https://doi.org/10.1007/s12665-019-8381-2>
- NorouziFriedmanPohn DWJDHA (1976) Lineament, linear, lineation: some proposed new standards for old terms. *Geol Soc Am Bull* 87(10):1463–1469. [https://doi.org/10.1130/0016-7606\(1976\)87%3c1463:LLSPN%3e2.0.CO;2](https://doi.org/10.1130/0016-7606(1976)87%3c1463:LLSPN%3e2.0.CO;2)
- Osmani SAH, Patil PH (2019) Drought response and relief by Jaldoot Express: a case study in Latur drought 2016. *Zenith IJMR* 9(6):224–236

- Ostad-Ali-Askari K, Shayannejad M, Ghorbanizadeh-Kharazi H (2017) Artificial neural network for modeling nitrate pollution of groundwater in marginal area of Zayandeh-rood River, Isfahan, Iran. *KSCE J Civ Eng* 21(1):134–140. <https://doi.org/10.1007/s12205-016-0572-8>
- Pande CB, Moharir KN, Singh SK, Varade AM (2020) An integrated approach to delineate the groundwater potential zones in Devdari watershed area of Akola district, Maharashtra, Central India. *Environ Dev Sustain* 22(5):4867–4887. <https://doi.org/10.1007/s10668-019-00409-1>
- Patra S, Mishra P, Mahapatra SC (2018) Delineation of groundwater potential zone for sustainable development: a case study from Ganga Alluvial Plain covering Hooghly district of India using remote sensing, geographic information system and analytic hierarchy process. *J Clean Prod* 172:2485–2502. <https://doi.org/10.1016/j.jclepro.2017.11.161>
- Pius A, Jerome C, Sharma N (2012) Evaluation of groundwater quality in and around Peenya industrial area of Bangalore, South India using GIS techniques. *Environ Monit Assess* 184(7):4067–4077. <https://doi.org/10.1007/s10661-011-2244-y>
- Rahmati O, Pourghasemi HR, Melesse AM (2016) Application of GIS-based data driven random forest and maximum entropy models for groundwater potential mapping: a case study at Mehran Region, Iran. *Catena* 137:360–372. <https://doi.org/10.1016/j.catena.2015.10.010>
- Razandi Y, Pourghasemi HR, Neisani NS, Rahmati O (2015) Application of analytical hierarchy process, frequency ratio, and certainty factor models for groundwater potential mapping using GIS. *Earth Sci Inform* 8(4):867–883. <https://doi.org/10.1007/s12145-015-0220-8>
- Razavi-Termeh SV, Sadeghi-Niaraki A, Choi SM (2019) Groundwater potential mapping using an integrated ensemble of three bivariate statistical models with random forest and logistic model tree models. *Water* 11(8):1596. <https://doi.org/10.3390/w11081596>
- Saaty TL (1980) *The analytic hierarchy process*. McGraw-Hill International, New York
- Saaty TL (2005) *Theory and applications of the analytic network process: decision making with benefits, opportunities, costs, and risks*. RWS publications, Pittsburg
- Saha R, Mitran T, Mukherjee S, Das IC, Kumar KV (2021) Groundwater management for irrigated agriculture through geospatial techniques. *Geospatial technologies for crops and soils*. Springer, Singapore. https://doi.org/10.1007/978-981-15-6864-0_13
- Saha R, Kumar GP, Pandiri M, Das IC, Rao PN, Reddy KSN, Kumar KV (2018) Knowledge guided integrated geo-hydrological, geomathematical and GIS based groundwater draft estimation modeling in Budhan Pochampalli watershed, Nalgonda district, Telangana State, India. *Earth Sci India* 11(4):216–231. <https://doi.org/10.31870/ESI.11.4.2018.14>
- Sahoo S, Dhar A, Kar A, Ram P (2017) Grey analytic hierarchy process applied to effectiveness evaluation for groundwater potential zone delineation. *Geocarto Int* 32(11):1188–1205. <https://doi.org/10.1080/10106049.2016.1195888>
- Shekhar S, Pandey AC (2015) Delineation of groundwater potential zone in hard rock terrain of India using remote sensing, geographical information system (GIS) and analytic hierarchy process (AHP) techniques. *Geocarto Int* 30(4):402–421. <https://doi.org/10.1080/10106049.2014.894584>
- Shufelt JA (1999) Performance evaluation and analysis of monocular building extraction from aerial imagery. *IEEE Trans Pattern Anal Mach Intell* 21(4):311–326. <https://doi.org/10.1109/34.761262>
- Singh A, Panda SN, Kumar KS, Sharma CS (2013) Artificial groundwater recharge zones mapping using remote sensing and GIS: a case study in Indian Punjab. *Environ Manag* 52(1):61–71. <https://doi.org/10.1007/s00267-013-0101-1>
- Singh A, Panda SN, Uzokwe VN, Krause P (2019) An assessment of groundwater recharge estimation techniques for sustainable resource management. *Groundw Sustain Dev* 9:100218. <https://doi.org/10.1016/j.gsd.2019.100218>
- Singha SS, Pasupuleti S, Singha S, Singh R, Venkatesh AS (2019) Analytic network process based approach for delineation of groundwater potential zones in Korba district, Central India using remote sensing and GIS. *Geocarto Int* 36(13):1489–1511. <https://doi.org/10.1080/10106049.2019.1648566>
- Sreedevi PD, Subrahmanyam K, Ahmed S (2005) Integrated approach for delineating potential zones to explore for groundwater in the Pageru River basin, Cuddapah District, Andhra Pradesh. *India Hydrogeol J* 13(3):534–543. <https://doi.org/10.1007/s10040-004-0375-8>
- Tamiru H, Wagari M (2022) Comparison of ANN model and GIS tools for delineation of groundwater potential zones, Fincha Catchment, Abay Basin, Ethiopia. *Geocarto Int* 37(23):6736–6754. <https://doi.org/10.1080/10106049.2021.1946171>
- Verma P, Singh P, Srivastava SK (2020) Development of spatial decision-making for groundwater recharge suitability assessment by considering geoinformatics and field data. *Arab J Geosci* 13(8):1–8. <https://doi.org/10.1007/s12517-020-05290-1>
- Zghibi A, Mirchi A, Msaddek MH, Merzougui A, Zouhri L, Taupin JD, Chekirbane A, Chenini I, Tarhouni J (2020) Using analytical hierarchy process and multi-influencing factors to map groundwater recharge zones in a semi-arid Mediterranean coastal aquifer. *Water* 12(9):2525. <https://doi.org/10.3390/w12092525>

Springer Nature or its licensor (e.g. a society or other partner) holds exclusive rights to this article under a publishing agreement with the author(s) or other rightsholder(s); author self-archiving of the accepted manuscript version of this article is solely governed by the terms of such publishing agreement and applicable law.